REPUBLIC OF TURKEY

YILDIZ TECHNICAL UNIVERSITY

GRADUATE SCHOOL OF NATURAL AND APPLIED SCIENCES

ENCAPSULATION OF LEMONGRASS OIL FOR ANTIMICROBIAL AND BIODEGRADABLE FOOD PACKAGING APPLICATIONS

Fidan Özge CAN

DOCTOR OF PHILOSOPHY THESIS

Department of Chemical and Metallurgical Engineering

Food Engineering Program

Advisor

Assoc. Prof. Dr. M. Zeki DURAK

March, 2021

REPUBLIC OF TURKEY

YILDIZ TECHNICAL UNIVERSITY

GRADUATE SCHOOL OF NATURAL AND APPLIED SCIENCES

ENCAPSULATION OF LEMONGRASS OIL FOR ANTIMICROBIAL AND BIODEGRADABLE FOOD PACKAGING APPLICATIONS

A thesis submitted by Fidan Özge CAN in partial fulfillment of the requirements for the degree of DOCTOR OF PHILOSOPHY is approved by the committee on 12.03.2021 in Department of Chemical and Metallurgical Engineering, Food Engineering Program.

Assoc. Prof. Dr. M. Zeki DURAK

Yıldız Technical University

Advisor

Approved By the Examining Committee

Assoc. Prof. Dr. M. Zeki DURAK, Advisor
Yıldız Technical University _____

Assoc. Prof. Dr. Fatih TÖRNÜK, Member
Yıldız Technical University _____

Assoc. Prof. Dr. Filiz ALTAY, Member
Istanbul Technical University _____

Prof. Dr. Bülent ERGÖNÜL, Member
Celal Bayar University _____

Assoc. Prof. Dr. Salih KARASU, Member
Yıldız Technical University _____

I hereby declare that I have obtained the required legal permissions during data collection and exploitation procedures, that I have made the in-text citations and cited the references properly, that I haven't falsified and/or fabricated research data and results of the study and that I have abided by the principles of the scientific research and ethics during my Thesis Study under the title of Location Analysis of The Emergency Service Centers Of a Case Company supervised by my supervisor, Assoc. Prof. Dr. M. Zeki DURAK. In the case of a discovery of false statement, I am to acknowledge any legal consequence.

Fidan Özge CAN

Signature

Dedicated to my mom

ACKNOWLEDGEMENTS

A special thanks to my advisor, Assoc. Prof. Dr. Muhammed Zeki Durak, for his countless hours of reflecting, reading, encouraging, and most of the patients, throughout the entire process.

I would like to thank the jury members who had devoted their valuable time and efforts to my thesis and for agreeing to serve on my committee.

I would like to acknowledge and thank the faculty members and assistants of the Food Engineering Department at Yildiz Technical University for their kindness and providing any assistance requested. Special thanks to Duygu Özmen, Öznur Saroğlu, and Hatice Bekiroğlu for their support throughout the whole process.

Above anything else, I would thank my entire family for their supports, solidarity and patience during my studies. Thanks to my cat Juli for pulling an all-nighter with me next to my laptop and thanks to Taygun for making everything easier for me.

Fidan Özge CAN

TABLE OF CONTENTS

LIST OF SYMBOLS

L*	Brightness
C	Celsius degree
º	Degree
ε′	Dielectric constant
h	Hour
µg	Microgram
µL	Microliter
µm	Micrometer
µS	Micro Siemens
mL	milliliter
mPa	Millipascal
min	Minute
nm	Nanometer
%	Percentage
pH	Power of hydrogen
a*	Redness
b*	Yellowness

LIST OF ABBREVIATIONS

ATR-FTIR	Attenuated total reflectance – Fourier transform infrared spectrometer
CFU	Colony Forming Unit
DSC	Differential Scanning Calorimeter
FDA	The U.S. Food and Drug Administration
GC-MS	Gas Chromatography – Mass Spectrometer System
GRAS	Generally Recognized as Safe
Gt	Gelatin
LEO	Lemongrass Essential Oil
MBC	Minimum Inhibitory Concentration
MIC	Minimum Bactericidal Concentrations
PCL	Polycaprolactone
NA	Nutrient Agar
NB	Nutrient Broth
TFA	2,2,2- trifluoroacetic acid

LIST OF FIGURES

LIST OF TABLES

ABSTRACT

Encapsulation of Lemongrass Oil for Antimicrobial and Biodegradable Food Packaging Applications

Fidan Özge CAN

Department of Chemical and Metallurgical Engineering

Doctor of Philosophy Thesis

Advisor: Assoc. Prof. Dr. M. Zeki DURAK

In this study, lemongrass oil (LEO) was encapsulated into polymer solutions consisting of gelatin and polycaprolactone by electrospinning method and it was designed to be used as food packaging by giving the polymers antimicrobial properties. First, the microbial activity of LEO used was determined, and the minimum inhibitory concentration (MIC) and minimum bactericidal concentrations (MBC) against four different foodborne pathogens were determined. MIC values varied from 0.03-0.06 µL/m and MBC values ranged from 0.03 to 0.12 µL/mL. The chemical composition was determined by the GC-MS study and the purity of the LEO was verified. The experimental design was formulated and the polymer/LEO mixtures were prepared in the proportions determined in compliance with this design. Physical properties of these prepared polymer solutions, such as conductivity, surface tension, viscosity and dielectric constant, have been determined and their effect on the mean diameter of the fibers and fiber morphology have been investigated.

By measuring the fiber diameter and antimicrobial properties of the nanofibers obtained from solutions at different concentrations that required for experimental design, the optimum nanofiber was selected. The determined optimum nanofiber

(0.6 PCL-0.4 Gt-0.95 LEO) and Gt / (0-0.5-1LEO) nanofibers as edible food packaging was fabricated. Average diameter of nanofibers was found to be 110 $\pm$ 39 nm only for gelatin and it was observed that the diameter increased with increasing LEO amount. The optimum PCL / Gt and Gt nanofibers were found to have approximately 99% antimicrobial activity against *Salmonella* Typhimurium and *Staphlycococcus aureus* bacteria. The FTIR analysis revealed that polymers and LEO had been encapsulated without chemical interaction. In addition, the thermal properties of all components were examined. Finally, the fabricated antimicrobial nanofibers were coated on chicken breast samples, stored for 7 days at refrigerator temperatures and microbially monitored to determine the effect of the produced nanofiber on chicken shelf life as an application study.

Keywords: food packaging, electrospinned nanofibers, essential oil encapsulation, lemongrass oil, biodegradable packaging.

ÖZET

Limonotu Yağının Antimikrobiyal ve Biyobozunur Gıda Ambalajı Uygulamaları için Elektroeğirme Yöntemiyle Enkapsüle Edilmesi

Fidan Özge CAN

Gıda Mühendisliği Bölümü

Doktora Tezi

Danışman: Doç. Dr. M. Zeki DURAK

Bu çalışmada limon otu yağı (LEO), jelatin ve polikaprolaktondan oluşan polimer çözeltilerine elektroeğirme yöntemiyle enkapsüle edilmiş ve polimerlere antimikrobiyal özellik de kazandırılarak, gıda ambalajı olarak kullanılması için tasarlanmıştır. Öncelikle kullanılan LEO'nun mikrobiyal aktivitesi belirlenmiş, seçilen dört farklı gıda kaynaklı patojene karşı gösterdiği minimum inhibitör konsantrasyon (MIC) ve minimum bakterisidal konsantrasyonları (MBC) belirlenmiştir. MIC değerleri 0.03-0.06 µL/mL arasında değişirken, MBC değerleri 0.03 ve 0.12 µL/mL aralığında bulunmuştur. Ayrıca GC-MS analizi yapılarak kimyasal kompozisyonu belirlenmiş ve LEO'nun saflığı teyit edilmiştir. Deney tasarımı oluşturulmuş ve bu tasarıma göre belirlenen oranlarda polimer/ LEO karışımları hazırlanmıştır. Hazırlanan bu polimer çözeltilerinin iletkenlik, yüzey gerilimi, viskozite ve dielektrik sabiti gibi fiziksel özellikleri belirlenmiş ve oluşan nanoliflerin ortalama çapına ve lif morfolojisine etkisi incelenmiştir. Deney tasarımı için gereken farklı konsantrasyonlardaki çözeltilerden elde edilen nanolifler, lif çapı

ve antimikrobiyal özellikleri ölçülerek optimum nanolifin seçimini sağlamıştır. Belirlenen optimum nanolif (0.6 PCL- 0.4 Gt- 0.95 LEO) ve yenilebilir gıda ambalajı olarak kullanılmak üzere Gt/ (0-0.5-1LEO) nanolifleri üretilmiştir. Ortalama nanolif çapları sadece gelatin için 110 ± 39 nm bulunmuş ve artan LEO miktarıyla çapın da arttığı görülmüştür. Optimum PCL/Gt ve Gt nanoliflerin *Salmonella* Typhimurium ve *Staphlycococcus aureus* bakterilerine karşı antimikrobiyal etkinliğinin yaklaşık 99% bulunmuştur. Yapılan FTIR analizi sonucunda polimerler ile LEO'nun kimyasal etkileşime girmeden enkapsüle edildiği görülmüştür. Ayrıca tüm bileşenlerin termal özellikleri de incelenmiştir. Son olarak bir uygulama çalışması yapılarak üretilen antimikrobiyal nanolifler tavuk göğsü örneklerine kaplanıp 7 gün boyunca buzdolabı koşullarında depolanarak ve mikrobiyal olarak izlenerek üretilen nanolifin tavuk raf ömrüne etkisi belirlenmiştir.

Anahtar Kelimeler: gıda ambalajı, elektroeğrilmiş nanolifler, esansiyal yağ enkapsülasyonu, limon otu yağı, biyobozunur ambalaj.

1
INTRODUCTION

1.1 Literature Review

Microbial contamination can decrease the shelf life of food and raise the risk of foodborne diseases. Fabrication of antimicrobial packaging materials is necessary for the food packaging industry in order to prevent and/or control foodborne diseases and improve food quality and shelf-life (Ardekani-Zadeh & Hosseini, 2019). The food packaging industry has started to benefit from the advantages of nanotechnology in order to avoid environmental issues that have risen in recent years, to meet customer demands and to keep up with emerging trends. One of these nanotechnology applications is electrospinning technology (Bhushani & Anandharamakrishnan, 2014).

Electrospinning is a novel high electric field-based technology that can be used to manufacture polymer and bio-polymer based ultrathin nanofibers. It has been shown that electrospun mats have specific features resulting from the very broad surface-to-volume ratios of nanofibers, the use of functional and/or recycled polymers or the encapsulation of bioactive compounds (Torres-Giner, 2011). The main advantages of this technology are its simplicity, low cost, and a promising continuous fiber production. As the electrical force is sufficiently applied to the droplet, the liquid overcomes the surface tension and becomes charged, the charged polymer is expelled from the Taylor cone, so that the fiber can be manufactured. Various process variables, such as the characteristics of polymer solutions (e.g. polymer type and concentration, viscosity, conductivity, surface tension, and solvent polarity), processing conditions (e.g., flow rate, voltage, and distance between the needle and collector) and environmental factors (temperature and humidity) have a significant effect on the fiber morphology. The electrospun fiber mats are used in the field of food packaging to serve as intermediate or coating layers to improve physical performance, including barrier properties, while serving as natural

connectors at the same time and can be functionalized by various active agents (Zhang, Li, Wang, & Zhang, 2020).

The U.S. Food and Drug Administration (FDA) classifies essential oils (EOs), which are natural antimicrobials, as Generally Recognized as Safe (GRAS). Thus, EOs are authorized for use in edible food packaging to enhance both the antimicrobial properties and hydrophilicity of polymer based packaging (Tang et al., 2019). Lemongrass essential oil (LEO) has been proved with excellent antimicrobial activity against a variety of pathogen, fungi and yeast (Han Lyn & Nur Hanani, 2020). The main component of lemongrass oil is citral (3,7-dimethyl-2,6-octadienal) which consists of two geometrical isomers, geranial (trans-citral) and neral (cis-citral). Citrals have been noted for their high antimicrobial activity, but are poorly water soluble and lose their therapeutic properties when exposed to sun, light and air. Therefore, encapsulation is a promising approach for improving EOs stability and allowing the preservation of biological properties over time (Riquelme, Herrera, & Matiacevich, 2017). Encapsulation of EOs by electrospinning can be used as active packaging material due to such benefits as the ability to control the release of the active material, the ratio of surface to volume, etc. (Kayaci, Sen, Durgun, & Uyar, 2014).

1.2 Objectives of the Thesis

This research aims to fabric electrospun composite which will consist of lemongrass essential oil and PCL and/or Gelatin as a polymer. One of the objectives of the study is optimizing the LEO/polymer/solvent ratio for smooth and homogenous diametered fibers. In order to obtain the desired antimicrobial properties for food packaging, a sufficient amount of lemongrass essential oil was encapsulated. An experimental design was created to optimize the components and determine the optimum polymer and essential oil mix for this aim. Characterization and analysis of the packaging material are other objectives. An application study on pieces of chicken breast and storage studies were conducted. The main goal is fabricating bioactive antimicrobial food packaging that is effective on determined spoilage or/and pathogen microorganisms and helps to prolong shelf life and maintain the quality of food products.

1.3 Hypothesis

In the literature, the electrospinning process has an increasing trend in the manufacture of antimicrobial and biodegradable packaging. It is possible to increase the shelf life and quality of food by using this type of packaging material.

This thesis consists of two different hypotheses. Firstly, it is hypothesized that electrospinning is an efficient method for the manufacture of antimicrobial food packaging material. Lemongrass oil (LEO) is an effective antimicrobial agent that can be used for this purpose. Another hypothesis tested in this thesis is that coating chicken breast samples with lemongrass oil encapsulated nanofibers would reduce the microbial load and prolong the shelf life of chicken breasts.

The findings of this study would help to pave the road for future applications of LEO encapsulated nanofibers in the food industry. This study will also contribute to the literature in terms of LEO encapsulated nanofiber characterization, antimicrobial efficiency and thermal stability of the packaging material. It will be possible to extend the shelf life of food without altering its quality in a natural way and will also help to reduce environmental pollution, which has recently become a significant concern.

2
GENERAL INFORMATION

2.1 Encapsulation

Encapsulation can be described as a method wherein one material (active agent) is enclosed inside another substance (wall material). The aim of encapsulation is to preserve the components from the atmosphere or environment, stabilization, and slow release of food ingredients (Gibbs, Kermasha, Alli, & Mulligan, 1999; Shahidi & Han, 1993). Fats and oils, oleoresin, aroma compounds, proteins, minerals, and enzymes have been encapsulated in the food industry so far. Encapsulated substances in the food industry have a multitude of potential benefits. Encapsulation of bioactive compounds allows food to be protected from environmental factors such as light, moisture, oxygen and heat during processing, storage and transportation. In addition, the encapsulation method has advantages such as preserving the physical properties of the active ingredients, masking the taste and odor thanks to the coating material, preventing adverse reactions with other ingredients, and allowing active ingredients to be used effectively in a small amount (Fathi, Martín, & McClements, 2014; Madene, Jacquot, Scher, & Desobry, 2006).

Many substances may be used to coat or encapsulate active materials. However, regulations for food additives are more restrictive than the other intended applications such as drug delivery systems. Compounds to be used in the food industry should be generally recognized as safe (GRAS) materials and the requirements of governmental organizations should be fulfilled (Wen, Zong, Linhardt, Feng, & Wu, 2017). The methodology of encapsulation and coating materials are interrelated. The required process or coating material is chosen based on the coating material or the methodology. Coating materials may be chosen from natural or synthetic polymers, depending on the material to be encapsulated. Chemical modifications to current coating materials are often considered for the purpose of modifying their properties. As compared to the existing coating

materials, these modified coating materials show improved mechanical and physical characteristics (Desai & Park, 2005).

Encapsulation Types

- Nanoencapsulation (less than 200 nm = 0.2 μm)
- Microencapsulation (0.2-5,000 μm)
- Macroencapsulation (greater than 5,000 μm) (King, 1995)

2.2 Encapsulation Techniques

Different approaches were proposed to encapsulate bioactive molecules, each with its own strengths and demerits. These techniques include freeze drying, spray drying, emulsification, inclusion complexification, nano-precipitation, and supercritical fluid, etc. (Wen et al., 2017). As the core material is mostly liquid, the encapsulation technology used is based on the drying principle. The choice of the most effective approach depends on the physical and chemical properties of the active compound and the polymer (coating material) to be coated (Poshadri & Aparna, 2010).

The spray drying process is the most preferred, cheapest and fastest system used for encapsulation in the food industry. In addition to energy loss during the spray drying process, food compounds such as essential oils and probiotics that are sensitive to heat due to the use of high temperatures may also be damaged (Koc, Sakin & Kaymak, 2010). For these reasons, interest in various methods, such as electrospinning, has recently increased, especially in the encapsulation of heat sensitive foods.

2.3 Electrospinning Method

Electrospinning is an easy and versatile process in which solid fibers are produced from a polymer solution or polymer melt delivered through a needle or a nozzle. It is a method that does not require heat, has a low cost and provides high encapsulation efficiency to obtain nanofiber from several different polymer types (Tian et al., 2011). Electrospun nanofibers have a high surface-to-volume ratio and very small pores; these characteristics make them useful in a variety of fields such

as tissue engineering, textile engineering, filtration, biomedical, pharmaceutical, optoelectronics, health, biotechnology, safety and environmental engineering, and food engineering (Shuiping, Lianjiang, Weili, Xiaoqiang & Yanmo, 2010). The materials used for the delivery of bioactive compounds by electrospinning are natural polymers or biodegradable synthetic polymers. Protein (gelatin, zein, casein etc.), carbohydrate (cellulose, chitin, alginate) and lipid (phospholipid) based natural polymer is more preferred because it is compatible with food. In this sense, they provide controlled and continuous release of active compound by encapsulating it with natural polymers (Bhushani & Anandharamakrishnan, 2014; Garcia-Moreno et al., 2016). In electrospinning technology, the properties of the active compound and the coating polymer and their behavior towards each other have an effect on the performance of the encapsulation process (Bhushani & Anandharamakrishnan, 2014).

2.3.1 History of Electrospinning

In the 17th century, William Gilbert revealed that electromagnetic forces had an influence on liquids and that his experiments were carried out by Lord Raleigh in the late 19th century. During the electrospraying process, considering the basic logic of electrospinning, the amount of load required for the uninterrupted flow of the solution was modeled by Lord Raleigh. Zeleny made major contributions to electrospraying in the first quarter of the 20th century. (Tucker, Stanger, Staiger, Razzaq & Hofman, 2012).

Some of the most important contributions to understanding electrospinning are provided by Taylor who demonstrated the formation mechanism of the jet in detail. He explained how the polymer droplet moves under electric field in 1969. According to these studies, when electrostatic forces and surface tension balanced, the drop on the needle tip takes on a conical structure, which is called the "Taylor Cone". At steady state, the apex angle of this cone is 98.6 ° (half angle 49.3 °). This situation explains how the diameter of the formed fibers is significantly smaller depending upon the diameter of the needle used (Sill & Recum, 2008). In the light of these studies, has been begun to generate nanofibers of various diameters after 1990 by electrospinning (Rutledge & Fridrikh, 2007).

2.3.2 Basic Principle of Electrospinning

The electrospinning assembly consists of a syringe pump, a high voltage power supply (5-60 kV) and a grounded metal collector plate (Fig 2.1). During the electrospinning process, the prepared polymer solution is injected into the syringe and the solution is supplied to flow at a steady flow rate with the power of the pump. During the operation, high voltage is generated between the collector plate and the tip of the syringe. As the polymer solution reaches the critical voltage value, the surface tension of the polymer solution and the electrostatic forces shall be equalized and the polymer droplet will take the form of a Taylor cone Nanofibers of various diameters are formed on the collector plate after the critical voltage value has been exceeded (Ghorani & Tucker, 2015; Park, 2011).

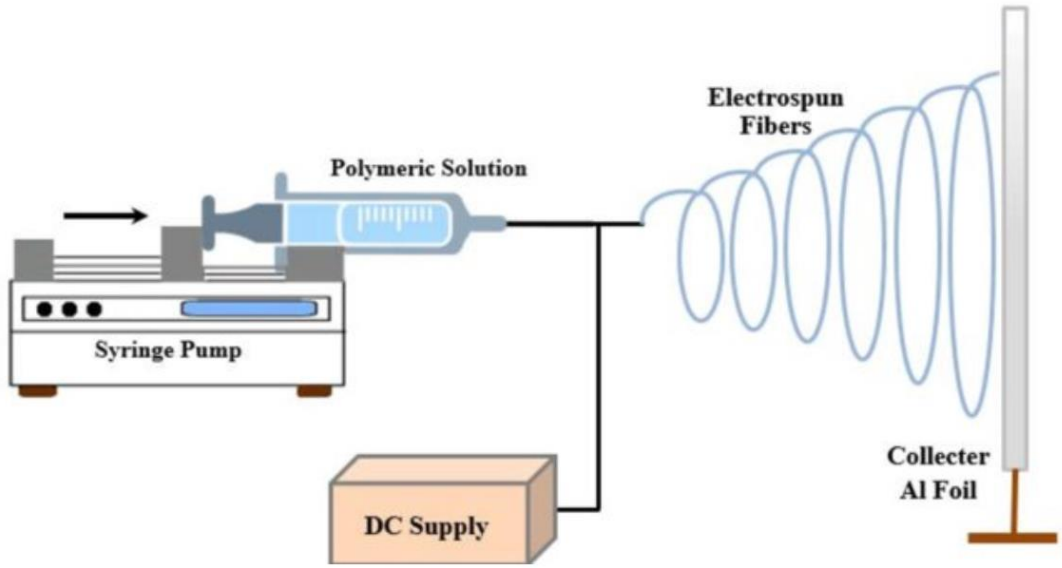

Fig 2.1 Schematic view of Electrospinning Process (Alharbi, Alarifi, Khan & Asmatulu, 2016)

The diameter of the fibers varies between micrometers and nanometers (Okutan, Terzi & Altay, 2016). Fiber diameters can be adjusted by changing process parameters. Factors that affect this process: Process parameters (flow rate, applied voltage, distance between the collector and the needle tip), Polymer properties

(concentration, viscosity, dielectric constant, molecular weight, surface tension, conductivity) and environmental factors (Schiffman & Schauer, 2008).

2.3.3 Affecting Parameters of Electrospinning Process

2.3.3.1 Process Parameters

2.3.3.1.1 Applied Voltage

A certain voltage must be applied to the solution for electrospinning to take place. As the applied voltage is high enough to surpass the surface tension of the polymer solution, a semi-stable, flat, electrically charged jet is formed at the tip of the needle that is attached to the electrode (Zong, Kim, Fang, Ran, Hsiao & Chu, 2002). At values below critical voltage, the solution does not take the form of a Taylor-cone at the tip of the syringe and the formation of fiber does not occur. At values above the critical voltage, there will be more charge accumulation in the solution, causing a longer and unstable jet formation. Rising the voltage provides thinning in the fiber size up to a certain point, but after a certain point causes the formation of a thick beaded structure as a result of drawing more polymer (Sill & Recum, 2008; Zong et al., 2002).

2.3.3.1.2 Flow Rate

Flow rate plays a role in determining the number of nanofibers to be formed per unit time. As the flow rate increases, the drop mass also increases; when polymer solution flowing from the tip of the needle to the collector plate, not all solvents will evaporate, and this increased flow rate will cause thicker fibers and beads (Sill & Recum, 2008).

When the flow rate is lower than required, due to the limited volume of polymer solution drawn, problems arise and Taylor cone cannot form continuously (Yarin, Koombhongse & Reneker, 2001).

2.3.3.1.3 Distance Between the Syringe and the Collector

One of the factors affecting the electrospinning process is the distance between the collector plate and the syringe tip. The distance should be adjusted to create a jet and allow the solvent to evaporate. Polymer solutions formulated with low-volatility

solvents need more distance to achieve smooth fiber than those formulated with high volatility (Subbiah, Bhat, Tock, Parameswaran & Ramkumar, 2005). As the evaporation time would be shorter if the distance is too short, this creates instability in the formation of Taylor cone and the formation of beaded nanofibers. If the distance is long, as the evaporation time will be longer, drier and smaller diameter fibers will be obtained (Ghorani & Tucker, 2015; Bhardwaj & Kundu, 2010).

2.3.3.2 Polymer Properties

2.3.3.2.1 Concentration

Polymer concentration determines the electrospinnibility of the solutions. Increased concentration causes an increase in fiber diameter. Low polymer concentration (due to low surface tension) causes beaded nanofiber structure (Subbiah et ai., 2015). High concentration of polymers makes the fiber formation challenging. Highly concentrated solutions accumulate at the tip of the syringe and prevents fiber formation or causes accumulation in a small area on the plate (Bhardwaj & Kundu, 2010).

2.3.3.2.2 Conductivity

Electrical conductivity is one the most important parameters for electrospinnibility. The polymer jet can be formed and stretched by the flow of charges on the surface of the jet. As the solution conductivity increases, the polymer loading capacity of the jet will also increase. As a result, under the same electric field, polymer jet with higher conductivity will be exposed to greater tensile force and a finer fiber will be obtained (Sill & Recum, 2008).

2.3.3.2.3 Surface Tension

As the surface tension of the polymer solution used increases, the tension needed for the forming of nanofiber increases. The surface tension of the polymer solution generally decreases with increasing polymer concentration. The high surface tension causes the formation of jet irregularity and beaded structure and stops the electrospinning process. Thinner and bead-free fiber formation is observed when surface tension is low. However, this does not mean that any polymer with low surface tension can be electrospun (Okutan et al., 2014).

2.3.3.2.4 Molecular Weight of Polymer Solution

As the molecular weight of the polymer that used for electrospinning increases, the length of the polymer chain and hence inter-chain interactions also increase. Through this increase, the structure of the fiber becomes relatively thicker, and the beads reduces or disappears (Bhardwaj, Kundu, 2010).

2.3.3.3 Environmental Factors

The temperature and relative humidity of the atmosphere can be viewed as important environmental factors in electrospinning. As the ambient temperature at which electrospinning takes place is increased, the viscosity of the polymer solution decreases. This condition will usually lead to a thinning of the fibers (Ziğal, 2012). Changes in relative humidity affect fiber diameter and drafting performance. Due to the decrease in the electrostatic force on the jet surface with the increase of relative humidity, the porous structure of the fibers on the collector plate and increasing fiber diameter is observed (Bhardwaj, Kundu, 2010).

2.4. Food Packaging Applications of Electrospinning Method

Production of antimicrobial packaging materials is essential for the food industry to prevent food-borne diseases and improve food quality and shelf-life (Ardekani-Zadeh & Hosseini, 2019). Components commonly used in the food packaging industry are mostly non-biodegradable plastics dependent on petrochemicals, which is one of the major contributors to environmental problems (Tang et al., 2019). The increase in consumers' demand for natural foods has led companies and researchers to investigate the natural and safe food packaging as well. Biodegradable polymers have been used as a replacement for synthetic plastic and have gained worldwide popularity in recent years due to their benefits over synthetic polymers. The major benefit of edible polymers over conventional polymers is that they can be eaten with the foods. Even if the package is not eaten, the waste can still be reduced as it is made of biodegradable material and this creates a safe perception for consumers (Shit & Shah, 2014).

Another use of electrospinning in food industry is active food packaging. The desired property of food can be preserved thanks to the active food packaging. For example,

moisture absorber, oxygen scavenger, antimicrobial agent releasing. Antimicrobial food packaging is also considered as active packaging (Echegoyen, Fabra, Castro-Mayorga, Cherpinski & Lagaron (2017). It is designed to extend the shelf life of food by incorporating antimicrobial properties to polymers that do not naturally have antimicrobial properties. The type and quantities of the active substance to be used and the properties of the polymer and whether it reacts with the active substance are also important for the design of antimicrobial food packaging (Sánchez-González, Vargas, González-Martínez, Chiralt & Chafer, 2011).

2.5. Encapsulation of Essential Oils for Food Packaging Applications

In the literature, there are plenty of study about various essential oils have been encapsulated with a wide variety of polymers and designed as food packaging. Tavassoli-Kafrani et al. (2018) used the electrospinning method to encapsulate orange essential oil into cross-linked gelatin nanofibers. Different ratios of essential oils were incorporated into gelatin nanofibers. With regard to the encapsulation efficiency and oil content of the fibers, the optimum ratio of gelatin or crosslinked gelatin to EO was found at 87:13. There was no significant change in nanofiber diameters with and without EO. A slight increase was observed in mean diameters of EO added fibers.

Lin et al. (2018) investigated the effect of thyme essential oil incorporated with gelatin nanoparticles and nanofibers on the shelf life and physicochemical properties of chickens. *Campylobacter jejuni* was selected as a target pathogen. The antimicrobial activity of these nanoparticles and nanofibers against *Campylobacter jejuni* was found to be very high. In addition, the morphology of the fibers produced by FTIR was examined. Finally, the oxidation degree, pH value and color analysis of chickens were made and this product was proposed as the new packaging material.

Wen et al. (2016) was produced the electrospun polyvinyl alcohol/cinnamon essential oil/β-cyclodextrin antimicrobial nanofibrous scaffolds with a mean diameter of 240 $\pm$ 40 nm. ATR-FTIR and thermogravimetric analysis revealed that the CEO was encapsulated in the cavity of β-CD and that there was molecular interaction between PVA, CEO and β-CD. Water contact angle analysis showed that CEO give hydrophobic characteristic to the film. The nanofiber film was tested on

strawberries. Antimicrobial and physicochemical properties of strawberries were observed during the storage. The packaging produced has been proven to increase the shelf life of strawberries.

Cinnamaldehyde was successfully integrated into chitosan/poly (ethylene oxide) solutions with a fiber diameter of 50 nm using electrospinning method by Rieger et al (2014). The outcomes of NMR analysis verified by release test wherein the cinnamaldehyde mats of 5 percent released a significantly higher amount of liquid cinnamaldehyde 545% more) and vapor form (279% more) than the 0.5 percent of cinnamaldehyde. The controlled release of cinnamaldehydes from nanofiber mats clearly affected their cytotoxicity against *P. aeruginosa.* This research offers prospects as a scaffold capable of alleviating nosocomial infections by providing a controlled release of broad-spectrum antibacterial agent.

Fonseca et al. (2020) analyzed the thermal properties of the nanofibers with a diameter of approximately 87-110 nm, which they fabricated using potato starch and thyme essential oil (TEO). According to the results of the TGA analysis, the thermal decomposition temperature of free TEO was found to be 62.1° C when it was 269.2 ° C after encapsulation, which indicates the improved thermal stability of the EO. They also conducted an antioxidant study and found that the tolerance of thyme essential oil to oxidative degradation improved when encapsulated.

2.6 Essential Oils

Essential oils are secondary metabolites derived from plants. They are secreted to protect plants from environmental hazards and diseases such as fungal and/or bacterial. Essential oils are biosynthesized, gathered and stored in special histological structures known as glands. The chemical composition, quantity and other properties of the essential oils differ according to the characteristics of the region in which they grow, the composition of the soil and its age (El Asbahani et al., 2015). Chemically, essential oils contain 85-99% volatile and 1-15% non-volatile components and are a mixture of hydrogenated and oxygenated monoterpenes, sesquiterpenes, phenols, simple alcohols, ketones, etc. which are all characterized by low molecular weight (Vishwakarma, Gautam, Babu, Mittal & Jaitak, 2016).

Essential oils have approved as generally recognized as safe (GRAS) by FDA. EOs have been commonly used in foods and pharmaceutical products for many years due to their antimicrobial features (Thang et al., 2019). Essential oils have a broad-spectrum antimicrobial effect, including bacterial, fungal. This powerful effect is usually provided by phenols and oxygen terpenoids. Compounds such as terpenes, esters and geranyl acetate, on the other hand, show weaker antimicrobial activity (Rao, Chen & McClements, 2019). The mechanisms of action of essential oils demonstrate their antimicrobial activity by entering and destroying the outer membranes of the bacterial cell. The hydrophilic lipopolysaccharide layer in the gram-negative bacteria cell wall membrane shows higher tolerance by forming an additional physical barrier (Vilela, Martins, Monteiro- Silva, Gonzalez-Aguilar & Almeida,Saraiva, 2016). Since the hydrophilic lipopolysaccharide layer of gram-negative bacteria in the outer cell wall membrane provides an extra physical barrier, they display higher tolerance compared to gram-positive bacteria. While most compounds present in essential oils have been characterized as antioxidants in in vitro tests, depending on the concentration, they may be cytotoxic but not genotoxic in general (Vilela et al., 2016).

2.6.1 Lemongrass Essential Oil

Lemongrass oil is an essential oil extracted from the aerial constituents of the Poaceae family, Cymbopogon citratus. The plant has been commonly known for its medicinal and phytochemistry utility. It has noted for the insecticidal, antimicrobial and therapeutic properties of its oil and extracts (Oyedele, Gbolade, Sosan, Adewoyin, Soyelu & Orafidiya, 2002; Naik, Fomda, Jaykumar, & Bhat, 2010). Lemongrass has many applications in the pharmaceutical, cosmetics and food industries.

LEO is distinguished by a high citral (formed by neral-geranial isomers) content that is used as a raw material for the manufacture of ionone, vitamin A and beta-carotene (Tzortzakis & Economakis, 2007). Its antimicrobial activity due to citronelal and citral compounds, mainly. In addition to these two components, compounds in lower concentrations such as linalool, geraniol, ш-pinene and terpinene also increase the antimicrobial effect providing a synergistic effect (Mirghani, Liyana, & Parveen,

2012). According to a study conducted by Saikia et al. (2001) LEO has more antimicrobial effect than pure citral component.

LEO has been shown to be effective against many food-borne pathogens when incorporated into berries, fruit juices, ground beef, chocolate, or fish products. However, EOs also have undesirable characteristics for this use, such as volatility, chemical instability, taste and odor, and insolubility in water. Therefore, it may be used encapsulated with coating polymers (Salvia-Trujillo, Rojas-Grau, Soliva-Fortuny & Martin-Belloso, 2014).

2.7 Gelatin

Numerous vegetable and animal proteins, such as collagen, gelatin, soy protein, zein, wheat gluten, casein, and whey proteins, are widely used to produce biodegradable and/or edible films. Gelatin, as a natural protein-based biopolymer, has excellent properties in film formation. Gelatin-based films have been widely used as packaging material in the industry to maintain food quality and prolonging shelf life (Ramos, Valdes, Beltran & Garrigós, 2016).

Gelatin is consisting of 50.5% carbon, 17% nitrogen, 25.2% oxygen, and 6.8% hydrogen. Gelatin is a heterogeneous mixture of polypeptides composed of α-chains (one polymer/single chain), β-chains (two alpha-chains covalently crosslinked) and γ-chains (three alpha-chains covalently crosslinked). It is produced (by chemical denaturation) from the insoluble protein called collagen and is obtained from bones, skin and connective tissue (Hanani, Roos, Kerry, 2014). The use of by-products from the fishing industry for gelatin production has increased in recent years, however has a disadvantage compared to mammalian sources due to its rheological properties. The most important physical properties of gelatin are gel strength and viscosity. Gel strength, also known as the Bloom value, is a measure of the gelatin's stiffness, representing the average molecular weight of its constituents and typically between 30 and 300 blooms (Ramos et al., 2016).

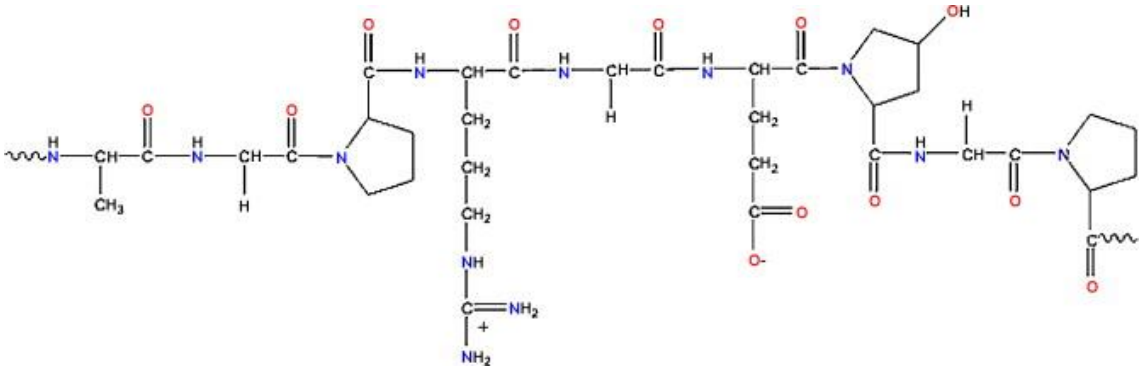

Fig 2.2 Gelatin Structure (Hanani et al., 2014)

Recently, the interest of customers in natural ingredients highlights gelatin as edible packaging material. In the literature, there are studies in which gelatin is dissolved with various solvents such as acetic acid and used in obtaining packaging by electrospinning method. Latest research has focused on methods like electrospinning for producing active films and coatings for food packaging, including antimicrobials, antioxidants and other agents that can improve the biological properties of food (Ramos et al, 2016; Wang, Liu, Li & Liu, 2015).

2.8 Polycaprolactone (PCL)

Due to its biocompatibility, mechanical properties and slow biodegradability, polycaprolactone (PCL) is one of the most widely used synthetic polymers for medicinal and packaging use (Van der Schueren, Schoenmaker, Kalaoglu & De Clerck, 2011; Labet & Thielemans, 2009). PCL is a semicrystalline linear aliphatic polyester, a valuable component in resorbable sutures, pharmaceuticals and bone graft replacements. In addition, PCL is one of the most hydrophobic of commercially manufactured biodegradable polymers, has good mechanical properties and is usually compatible with many forms of polymers (Elzein, Nasser-Eddine, Delaite, Bistac & Dumas, 2004).

Two major polycaprolactone production mechanisms have been identified: hydroxycarboxylic acid polycondensation: 6-hydroxyhexanoic acid, and lactone ring-opening polymerisation (ROP): ε-caprolactone (ε-CL). PCL is strongly soluble in chloroform, tetrachloride carbon, dichloromethane, benzene, toluene, cyclohexanone and 2-nitropropane; slightly soluble in 2-butanone, acetone, ethyl acetate, dimethylformamide and acetonitrile; and insoluble in diethylether,

petroleum ether, alcohols, and water at room temperature. Biodegradation of PCL occurs over a span of several months to several years depending on the degree of crystallinity and molecular weight of the polymer, and the deterioration states. Most microorganism in nature are able to fully biodegrade PCL (Labet & Thielemans, 2009).

3
EXPERIMENTAL STUDIES

3. 1 Materials and Methods

3.1.1 Research Plan

This study consists of four main parts.

The first part of the study was to determine the chemical and microbiological properties of lemongrass essential oil to be encapsulated. Its purity was confirmed by screening the chemical composition of lemongrass oil obtained from a reputable brand, and its microbial activity was determined.

The second part of the study was designing the experiment. Design Expert 7.0 was used to optimize the components and determine the optimum polymer mix for the electrospinning process. We had two components (Polycaprolactone, gelatin), one factor (lemongrass essential oil) and two responses (average diameter of nanofibers, antimicrobial activity). For this reason, 19 separate runs were carried out, and after determining the average diameter of nanofibers and the antimicrobial activity of all of them, nanofibers with optimum properties were selected.

In the third part, lemongrass essential oil loaded nanofibers were encapsulated into the mix of polycaprolactone (PCL) and gelatin (Gt) polymers by electrospinning method. Antimicrobial activity of the fabricated nanofibers was tested. Nanofibers were characterized by using Fourier-transform infrared spectroscopy (FTIR), Differential scanning calorimetry (DSC) and Scanning electron microscope (SEM).

As the fourth and the last part of the study, an experimental study was conducted. Chicken breast pieces were coated with optimum electrospun nanofiber mats that previously determined and the storage study was carried out. Microbial alterations in chicken samples have been observed for 7 days.

3.1.2 Materials and cultures

Lemongrass essential oil (LEO) was purchased online from Tisserand (West Sussex, England). As a natural water-soluble protein, gelatin bovine skin Type B with a bloom value of 225 (Sigma-Aldrich, St. Louis, MI, USA) was used. Poly-ε-caprolactone (PCL; Mn = 80,000, Sigma-Aldrich Co.) was another polymer. Acetic acid (Sigma-Aldrich) for gelatin and 2,2,2-Trifluoroethanoic acid (TFA) for PCL were used as solvents. The antimicrobial activity of the LEO was tested against four common microorganisms. The strains were *Staphylococcus aureus* ATCC 25923, *Escherichia coli* ATCC 25922, *Salmonella* Typhimurium *enterica* subsp. *enterica* ATCC 14028, and *Bacillus cereus* ATCC 14579. LEO encapsulated nanofibers were tested against *S.* Typhimurium ATCC 14028 and *S. aureus* ATCC 25923.

3.2 Screening of Lemongrass Essential Oil

3.2.1 Chemical Composition of Lemongrass Essential Oil

Tisserand brand organic lemongrass oil was purchased online.

Fig 3.1 Lemongrass Essential Oil

Headspace GC-MS analysis was performed in order to confirm chemical composition of LEO by using the GC-MS-QP2010 gas chromatography-mass spectrometer system (Shimadzu, Milan, Italy). Commercial libraries were used to identify the compounds detected. Instrument control and data collection were provided by GC-MS Solution software. 5000, 1000, 500, 250, 125, 62.5, 31.25, 15.625 ppm of LEO were dissolved

in 80% (w/w) ethanol, then the sample was held at 50°C for 1 min, 200 °C for 1 min and 300 °C for 30 min for separation of volatile components.

Fig 3.2 Gas Chromatography-Mass Spectrometer System (GCMS)

3.2.2 Determination of Antimicrobial Properties of Lemongrass Essential Oil

The antimicrobial activity of LEO was assessed against 4 food-borne pathogenic bacteria. The Gram-positive bacteria tested were *Staphylococcus aureus, Bacillus cereus,* and the Gram-negative bacteria were *Escherichia coli, Salmonella* Typhimurium. Agar well diffusion method was used to evaluate the antimicrobial activity of LEO. To maintain working culture, loopful portion of de-frozen bacterial cells were spread to Nutrient Agar (NA). Agar plates were incubated at 37°C for 24 h. After one day incubation, working cultures were stored in the refrigerator at 4°C. To maintain viability, sub-culturing was performed every 3 weeks. One day before the analysis, the bacteria on the agar plates were transferred to the nutrient broth and allowed to grow for a day at 37°C. For the analysis: First, 100 µL of each broth

culture was spread onto nutrient agar plates. Then, a hole with a diameter of 6 mm has punched aseptically and 10 µL of LEO pipetted into the well. Agar plates were incubated at 37 °C for 24 h for all the tested bacteria. The inhibition zones were measured in mm (Naik et al., 2010). The tests performed duplicate.

In order to assess the Minimum Inhibitory Concentration (MIC) and Minimum bactericidal concentration (MBC) values of LEO quantitatively, the broth dilution method was used. Sterile glass test tubes containing 0.5, 0.25, 0.125, 0.03, 0.015 mg LEO in 1 mL of Nutrient Broth (NB) was prepared and 1% Tween 80 solution was added as an emulsifier. 0.5 mL of the prepared solution was put into 4.4 mL NB and inoculated with 0.1 mL of overnight *S. aureus*, *B. cereus, E. coli*, and *S.* Typhimurium cultures. Then put into shaker incubator for 24 h at 37 °C. The tested bacteria were grown in Nutrient broth (NB) at 37 °C for overnight. MIC was regarded as the lowest concentration at which visible bacterial growth was not observed. MBC values were determined by seeding of 100 µL aliquots from the test tubes that showed no visible bacterial growth.

3.3 Experimental Design

In order to optimize LEO/PCL/Gt ratio for smooth, homogenous and bead-free fibers, an experimental design was created using Design Expert version 7 software (Stat-Ease Inc., USA). The parameters of the experimental design were as it follows: Component 1: Polycaprolactone (PCL), Component 2: Bovine Gelatin (Gt), Factor: Lemongrass essential oil (LEO), Response 1: Antimicrobial activity of the nanofibers, and Response 2: Average diameters of nanofibers. 19 different electrospinning runs were performed and the antimicrobial activity of the resulting nanofiber mat and the average of the fiber diameters were calculated.

Table 3.1 Experimental Design

Std	*Run*	*Block*	*PCL*	*Gelatin*	*Factor*	*R1*	*R2*
18	1	Block 1	1.00	0.00	0.00		
5	2	Block 1	1.00	0.00	0.00		
1	3	Block 1	0.50	0.50	0.50		
7	4	Block 1	1.00	0.00	0.50		
14	5	Block 1	1.00	0.00	0.25		
19	6	Block 1	0.50	0.50	1.00		
13	7	Block 1	0.25	0.75	0.75		
15	8	Block 1	0.00	1.00	1.00		
11	9	Block 1	0.75	0.25	0.75		
2	10	Block 1	0.00	1.00	0.50		
16	11	Block 1	0.00	1.00	0.00		
8	12	Block 1	0.00	1.00	0.00		
6	13	Block 1	1.00	0.00	1.00		
17	14	Block 1	1.00	0.00	1.00		
10	15	Block 1	0.75	0.25	0.25		
12	16	Block 1	0.25	0.75	0.25		
4	17	Block 1	0.50	0.50	1.00		
9	18	Block 1	0.00	1.00	1.00		
3	19	Block 1	0.50	0.50	0.00		

3.4 Preparation of Electrospinning Solution

Gelatin (Gt), as an electrospinning solution, (10%, w/v) was dissolved in a solvent consisting of acetic acid and distilled water at a ratio of 8:1 and was stirred at 50 °C for 1 h. A certain amount of LEO (0, 5, and 10%) was added to the mixture and was stirred for 3 h at room temperature using a magnetic stirrer.

Polycaprolactone (PCL) was another polymer that used in this study. 10% of PCL (w/v) was dissolved in 1,1,1- trifluoroacetic acid (TFA) and distilled water at a ratio of 8:1 and was stirred at the same temperature and time as gelatin solution.

For the mixture of Gt /PCL solutions, TFA, acetic acid and distilled water mixture used as a solvent. The ratio was changed depending on the component percentage.

3.5 Physical Properties of Feed Solutions

Electrospinnability of the polymer solution was investigated by measuring conductivity, viscosity, surface tension, and dielectric constant parameters.

The electrical conductivity of feed solutions was measured at room temperature in duplicates by a conductometer (WTW LF95, Germany). Viscosity measurements conducted with an air- bearing rheometer (Anton Paar, MCR-302) attached with paralel-plate geometry measuring equipment. In order to define the flow type, Power Law model is used. Shear rate and shear stress data that are acquired from the rheometer are used for regression analysis.

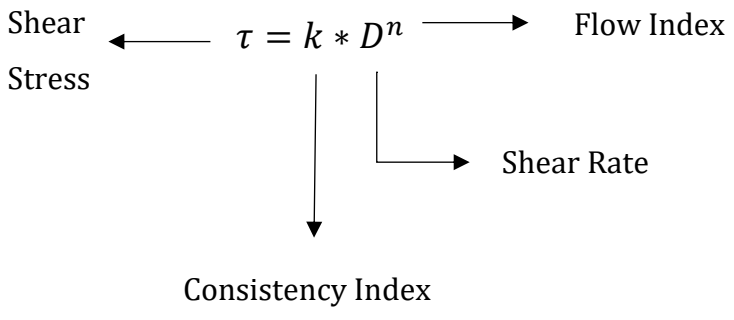

Figure 3.3 Viscosity of some food materials (Macosko, and Krieger ,1996)

Using n (flow index) value we can define the flow type of the material.

Flow types according to flow index:

n=1	Newtonian Flow
0<n<1	Psedoplastic Flow
n>1	Dilatant Flow

After determination of flow type, non-linear regression analysis was applied; shear rate vs shear stress data plotted and slope gave us the viscosity value.

The Wilhelmy plate method was used to measure the surface tension of the feed solutions by a tensiometer (Dataphysics DCAT 11EC, Germany).

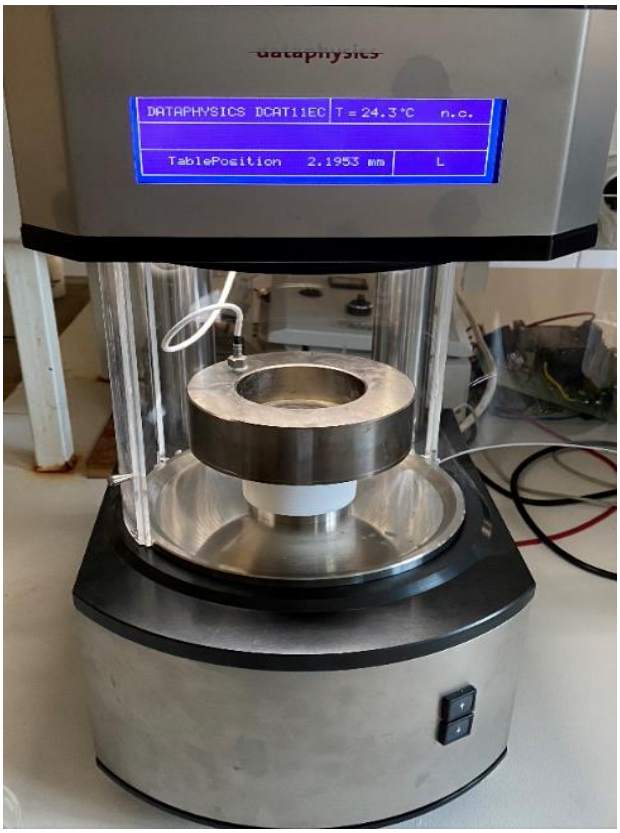

Fig 3.4 Tensiometer

A network analyzer (Agilent E5061 B, frequency range: 100 kHz – 3 GHz, USA) equipped with a dielectric probe kit was used to measure the dielectric constant of feed solutions at 25 °C in duplicate for each sample. Dielectric constants were measured at 3 GHz.

Fig 3.5 Network Analyzer

3.6 Electrospinning Process

Electrospinning was conducted in an ordinary electrospinning set up (Holmarc, Model No: HO-NFES-043U, India), which consisted of a 20 mL syringe with a needle filled with gelatin solution (0, 5, and 10% LEO), a syringe pump, a high voltage supplier (up to 30 kV) and a plate collector. The solution flow rate was set at 0.5 mL/h and the applied voltage was 19 kV. A collecting plate is covered by a piece of aluminum foil as the collector for the fiber deposition. The needle to the collector distance was 12 cm. Each process was conducted at 27 °C for 3h.

Fig 3.6 Electrospinning Unit

3.7 Fiber Morphology and Size Assessment

A scanning electron microscope (SEM, Carl Zeiss EVO LS 10, Germany) at an accelerating voltage of 10 kV under 10000 - 20000X magnification, was used to observe the morphology of the nanofibers. Samples were coated with electrically conductive Au-Pd under vacuum before analysis. The average diameter sizes of the fibers were evaluated by Image J 1.32 software (National Institutes of Health, Bethesda, MD, USA) by measuring 15 different diameter of nanofibers, and % distribution graphs were plotted using Origin (Pro) Version 9.0 (OriginLab Corporation, Northampton, USA).

3.8 Fourier Transform Infrared Spectroscopy (FTIR) of Nanofibers

FTIR analyses were performed in order to determine the possible chemical interactions among bovine gelatin, PCL and/ or LEO in the fibers. Characterization of chemical structure of pure LEO, and Gt/ PCL nanofibers with and without LEO were carried out with Bruker Tensor 27 spectrometer with a KBr beamsplitter and a DLaTGS detector (Bremen, Germany). In all the calculations, the diamond single-bounce ATR accessory was included. During the measurement, the crystal surface was wiped with ethanol in the transitions between samples. Data acquisition was achieved using OPUS Version 7.2.

3.9 *In vitro* Antimicrobial Efficiency of the Nanofibers

The efficiency of Gt / LEO nanofibers against *S.* Typhimurium as Gram-negative bacteria and *Staphylococcus aureus* as the Gram-positive bacteria was evaluated by the colony counting method according to the reference (Aytac, Ipek, Durgun, Tekinay, & Uyar, 2017) with slight modifications. *S.* Typhimurium and *S. aureus* cultures were grown in Nutrient Broth (NB) by incubating them at 37 °C for 24h. Serial dilutions of inoculum (10^1-10^9) were prepared with sterile peptone water (0.1w/v) and then 0.1 mL of samples from 10^4 to 10^9 dilutions pipetted onto Nutrient Agar (NA) plates in order to determine “A”. In order to calculate “B” 0.5 g of nanofiber samples were added in to NB tubes with 0.1 mL of inoculum. Incubation time for the plates was 24h at 37 °C. Then the colonies were counted and expressed

as CFU/mL. The antibacterial efficiency of the nanofibers was calculated using Eq. 3.1.

$$\text{Antibacterial efficiency (\%)} = 100\ (A - B) / A \qquad (3.1)$$

Where A and B is the number of colonies (CFU / mL) before and after electrospun fibers are added, respectively.

3.10 Differential Scanning Calorimetric (DSC) Studies

Differential Scanning Calorimetry (DSC) (Tzero Q2000, TA Instruments, New Castle, Del., U.S.A.) was used to study thermal properties of the samples. The temperature ranged between -85 °C to 160 °C, and the heating rate was 10 °C/min. Approximately 5 mg of the samples were sealed in an aluminum pan. An empty sealed pan was used as reference. Tests were duplicated.

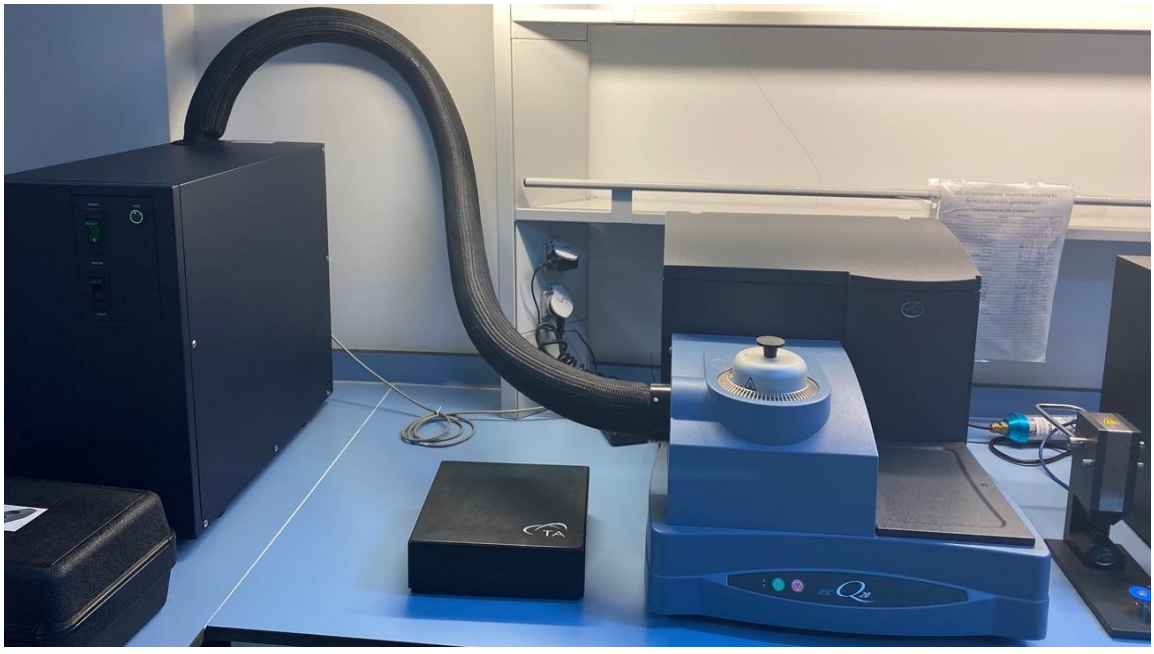

Fig 3.7 Differential Scanning Calorimetry (DSC)

3.11 Application Study

3.11.1 Determination of Physicochemical Properties

Chicken meat, which spoils quickly and causes economic losses in the industry, was selected for the application. The chicken breasts to be used for the study was purchased from a common chain store. Chicken breast samples were cut into 2x3

cm, approximately 10 grams, covered with optimum electrospun nanofibers and placed in petri dishes then stored at +4 ℃ for 7 days. Physicochemical analyzes were performed on the 0, 1st, 3rd, 5th, and 7th days of storage. Analysis was duplicated. Control (chicken samples without nanofibers) and optimum nanofibers coated chickens were the samples. The samples were weighed, 90 mL of distilled water was added, and the pH value was measured by a pH meter (Mettler Toledo, MP220, Switzerland).

To assess the color changes of the chicken samples, Chroma Meter-CR 400 (Konica Minolta, Japan) was used to measure the CEILAB where L* indicates the lightness, and a* indicates redness while b* indicates the yellowness of the samples. Two random spots were chosen on the chicken sample and analyzed. The variation of colors was calculated using the following equation:

$$\Delta E = (\Delta L^2 + \Delta a^2 + \Delta b^2)^{0.5} \quad (3.2)$$

Where; $\Delta L = L^* - L^*_{0.day}$, $\Delta a = a^* - a^*_{0.day}$, $\Delta b = b^* - b^*_{0.day}$ (Can, Demirci, Puri & Gourama, 2014).

3.11.2 Determination of Microbiological Properties

The microbiological properties of chicken meat pieces covered with electrospun nanofiber and the viability of inoculated *Salmonella* Typhimurium have been investigated.

Chicken breasts were cut into pieces (10 g), washed with sterile DI water and inoculated with 10 µL of *S.* Typhimurium using pipette then covered with electrospun fibers that previously fabricated for 3h. Baking paper was used to collect nanofibers in order to remove the produced nanofibers easily. LEO encapsulated nanofiber covered chicken samples were placed in sterile petri dishes and stored at 4 ℃ for a week. Microbiological analysis was performed on the 0., 1., 3., 5., and 7. days of storage. The study was duplicated. Salmonella-inoculated chicken breast samples were homogenized for 1 min after adding 90 mL of DI water

and dilutions were prepared up to 10^{-7}. 0.1 ml of the dilution was inoculated onto SS (Salmonella Shigella Selective) agar.

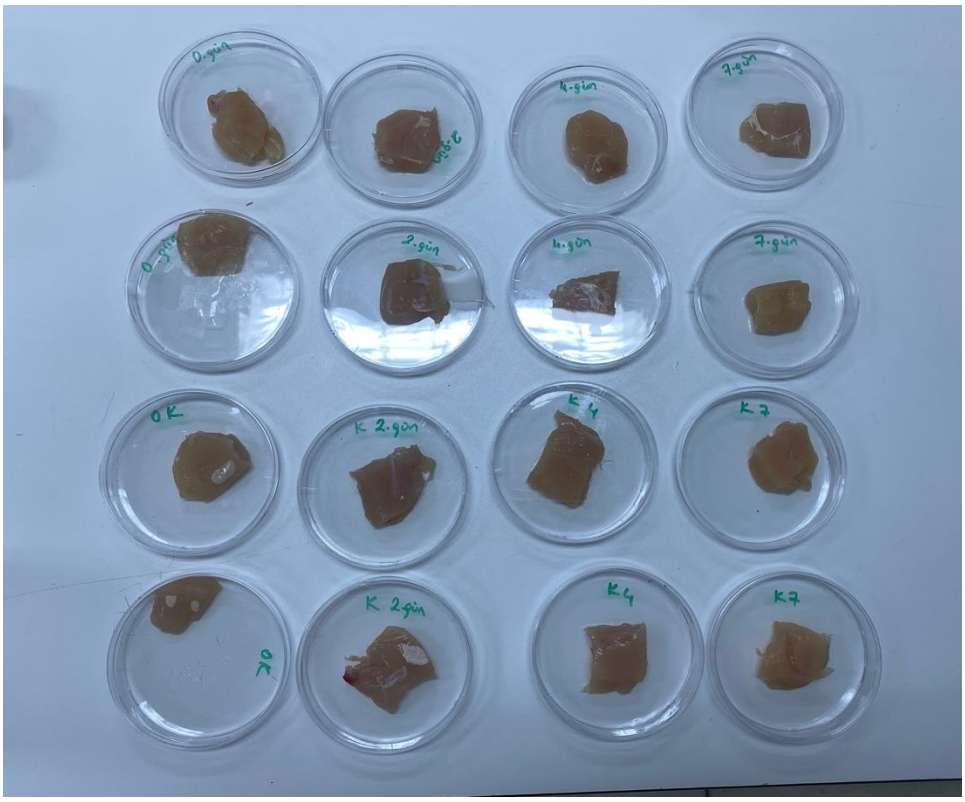

Fig 3.8 10 µL of *S.* Typhimurium inoculated chicken breast samples

3.12 Statistical Analysis

All experiments were conducted in duplicates, and the data were presented as mean ± standard deviation. The results were analyzed by one-way ANOVA using MINITAB (version 19, MINITAB, Inc., PA, USA). Using Tukey's method at the 95 percent confidence level, significant differences in mean values were calculated.

4
RESULTS

4.1 Essential Oil Screening

4.1.1 Chemical Composition of Lemongrass Essential Oil

In order to obtain a calibration graph (Fig 4.2) for GCMS analysis 5000, 1000, 500, 250, 125, 62.5, 31.25, 15.625 ppm of LEO were dissolved in 80% (w/w) ethanol, then the sample was held at 50°C for 1 min, 200 °C for 1 min and 300 °C for 30 min for separation of volatile components.

According to the headspace GC-MS analysis results, LEO consists of 25 components. The main components were citral (46.06%) and (Z)-citral (neral) (33.38%). Camphene (1.10%), 6-methyl-5-hepten-2-one (1.39%), 1,6-octadien-3-ol, 3,7-dimethyl- (1.62%), trans-caran, 4,5-epoxi- (1.57%), trans-geraniol (2.79%), 2,6-octadien-1-ol, 3,7-dimethyl-, acetate, (E)- (1.49%), and trans-caryophyllene (1.58%) were the components present in the LEO sample at a ratio of more than 1%. The presence of other components was less than 1% (Table 4.1). Some peaks of negligible amount of clearly non-LEO compounds were seen in Fig 4.2, which were omitted from the Table 4.1.

Mirghani et al (2012) determined the composition of LEO by GC-MS analysis in their bioactivity of lemongrass (Cymbopogan citratus) essential oil study. A total of 68 constituents from lemongrass leaves, and 72 from stalks of lemongrass were characterized. GC-MS analysis showed that geranials (32.10 % and 29.64 %), neral (22.36% and 21.73%), geraniol (5.40% and 7.75%), and limonene (5.71% and 5.92%) were found to be the major components of lemongrass essential oil.

Jumapaeng et al. found 49.40% trans citral and 27.48% cis citral to be the main components of LEO similar to our results (Jumepaeng, Prachakool, Luthria, & Chanthai, 2013). Priya et al. (2016) evaluated the chemical composition of LEO collected from three different locations in India. Z-citral and citral were also

determined as main components. Z-citral values were 10.61%, 23.17%, and 34.78% depending on the area (Yashaswini & Iyer, 2019).

When the studies in the literature are compared with our results qualitatively and quantitatively, the differences can be attributed to many reasons such as harvest maturity, genetic and environmental factors, extraction method and analysis methods (Asbahani et al., 2015).

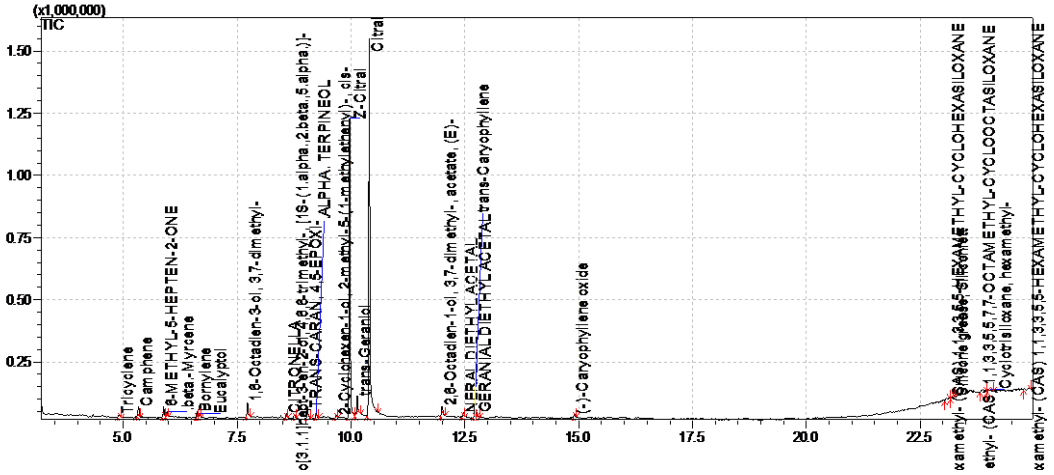

Fig 4.1 GCMS peaks of LEO

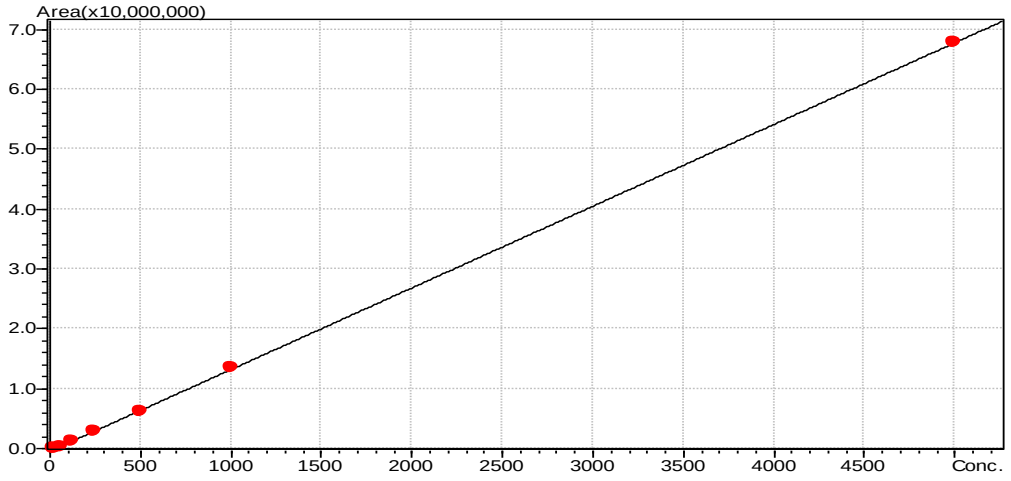

Fig 4.2 Calibration Graph for LEO

$Y = 13658.44X - 445498.1$

$R^2 = 0.9999174$

$R = 0.9999587$

Table 4.1 Composition of Lemongrass Essential Oil (LEO)

Compound	*Retention Time (min)*	*Concentration (%)*
Tricyclene	4.9	0.44
Camphene	5.3	1.10
6-Methyl-5-Hepten-2-One	5.8	1.39
Beta-Myrcene	5.9	0.64
Bornylene	6.6	0.65
Eucalyptol	6.7	0.48
1,6-Octadien-3-Ol, 3,7-Dimethyl-	7.7	1.62
Cıtronella	8.6	0.45
Bicyclo	8.8	0.55
Trans-Caran, 4,5-Epoxı-	9.0	1.57
Alpha. Terpıneol	9.2	0.54
2-Cyclohexen-1-Ol, 2-Methyl-5-(1-Methylethenyl)-, Cis-	9.7	0.39
Z-Citral	9.9	33.4
Trans-Geraniol	10.1	2.79
Citral	10.4	46.7
2,6-Octadien-1-Ol, 3,7-Dimethyl-Acetate, (E)-	12	1.49
Neral Dıethyl Acetal	12.5	0.56
Trans-Caryophyllene	12.7	1.58
Geranıal Dıethyl Acetal	12.8	0.63
(-)-Caryophyllene Oxide	14.9	0.40

4.1.2 Antimicrobial Properties of Lemongrass Essential Oil

Antimicrobial activity of the LEO was tested against the *Staphylococcus aureus, Bacillus cereus* as Gram-positive, and *Escherichia coli, Salmonella* Typhimurium as the gram-negative food-borne disease-associated bacteria with disc diffusion method, and Minimum Inhibitory Concentration (MIC) and the minimum bactericidal concentration (MBC) values were also determined (Table 4.2).

LEO was found effective against all the tested bacteria. *S. aureus* was the most sensitive bacteria to LEO among others and presented the largest inhibition zone (18 mm). Naik et. al (2010) evaluated different concentrations (5 %, 10 %, 15%, 20%, 25%, and 30 %) of lemongrass oil against some pathogenic bacteria and found that 30% LEO showed 29.66, 28.00, and 24.66mm inhibition zone against *S. aureus, B. cereus,* and *E. coli,* respectively. Gram-positive bacteria were more sensitive to LEO similar to our results. It has been demonstrated in studies that gram negative bacteria have an outer membrane surrounding the cell wall, limiting the diffusion of hydrophobic compounds (Burt, 2004).

Kotzekidou et. al (2008) tested the efficacy of different plant extracts and essential oils against *Bacillus cereus, Escherichia coli* O157:H7, *Salmonella* Typhimurium, *Staphylococcus aureus, Staphylococcus aureus* S-6, and *Listeria monocytogenes*. LEO showed 8.5, 0, 0, 15.2, 25.1, 15.2 mm of inhibition zones to the bacteria listed above, respectively. Our findings are similar, but only *B. cereus* strain showed 12 mm of inhibition zone in our study while they could not observe any zone. This may have been due to the difference between the strains of the bacteria used.

MIC and MBC values were also determined in our study. MIC was considered to be the lowest concentration at which no visible bacterial growth was observed. MIC value was 0.03 µL/mL for *S. aureus, B. cereus* and *S.* Typhimurium bacteria. *E. coli* showed no visible growth at 0.06 µL/mL of LEO concentration. After that, the MBC values were determined by seeding 100 µL aliquots from the test tubes which showed no visible bacterial growth. Our MBC values findings ranged between 0.03 and 0.12 µL/mL.

Table 4.2 Antimicrobial activity of LEO against different foodborne disease-associated bacteria, MIC and MBC values

Bacteria	Inhibition zone(mm)	(MIC (μL·mL^{-1})	MBC (μL·mL^{-1})
S. aureus ATCC 25923	18.0 ± 1.4	0.03	0.06
B. cereus ATCC 14579	12.0 ± 1.0	0.03	0.03
E. coli ATCC 25922	9.0 ± 1.2	0.06	0.12
S. Typhimurium ATCC 14028	10.0 ± 1.8	0.03	0.06

Naik et. al (2010) evaluated antimicrobial effect of LEO also. They found out that LEO was effective at much lower concentrations in the broth dilution method compared to the agar diffusion method. They determined the initial and final MIC and MBC values of *S. aureus* and *E. coli, B. cereus, B. subtilis, Klebsiella pneumoniae, Pseudomonas aeruginosa.* The MIC values they found for these bacteria are as follows, respectively: 0.03, 0.06, 0.03, 0.03, 0.25 and N.D. With the exception of *P. aeruginosa*, LEO was considered successful against all the microorganisms examined. Gram positive species were shown to be more susceptible than gram negative like the other studies. Their findings are very similar to ours; the MIC value of *B. cereus* were the same as our result. However, the MBC value for *B. cereus* (0.06) was slightly different from our result (0.03) (Naik et al., 2010).

Although the antimicrobial activities of essential oils are mostly determined by their main components, there is a complicated circumstance. We cannot attribute the antimicrobial effect of a complex mixture to a single substance. An antagonistic and synergistic effect can be observed between the components of the oil (Burt, 2004).

The antimicrobial features of LEO make it an important bacterial and fungal infection medicine. It is possible to wound cleansing and the treatment of fungal infections like a ringworm. It may also be used after food poisoning or bacterial infections in the colon, abdomen, and urinary tract (Singh, Singh, Singh & Ebibeni, 2011).

4.2 Physical Properties of Polymer Solutions

Conductivity, surface tension, viscosity and dielectric constant values of Polycaprolactone (PCL) and/or Gelatin (Gt) polymers with different concentrations of lemongrass essential oil (LEO) are given with the diameters of nanofibers fabricated from these solutions in Table 4.4.

It is well known that electrical conductivity, viscosity and surface tension are important parameters for electrospinnability and the morphology of the nanofibers. For nanofiber formation, a minimum electrical dope conductivity is required. The sort of solvent and polymer, polymer concentration, and temperature largely affect electrical conductivity (Mahmood, Kamilah, Sudesh, Karim & Ariffin, 2019). The electrical conductivity of the feed solutions was measured by a conductometer. It was 13.65 $\pm$ 0.13 µS/cm for pure Gt and 6.15$\pm$ 0.05 µS/cm for pure PCL solution and decreased by the addition of LEO. Similarly, Vafania et al. (2019) recorded that the electric conductivity of gelatin/chitosan (6:1) mix decreased with the increase of thyme essential oil. Silva et al. (2018) observed a similar decreasing trend in the electrical conductivity of solutions with the addition of ginger essential oil. They also noted that this decrease did not change the morphology of the fibers. Increased electrical conductivity of the solutions allowed the development of finer nanofibers for 2 reasons: 1) because of the higher electrical charge carried by the electrospinning jet, the higher elongation forces are applied. 2) Increased bending instability during electrospinning, allowed the jet path longer and fine nanofibers were obtained.

It is associated with the electrical charges on the solution exceeding the surface tension of the solution so that the electrospinning process can begin (Mendes, Stephansen & Chronakis, 2017). The lower surface tension spinning solutions provide uniform, bead-free fibers, but it does not mean that any solution with low surface tension can be electrospun (Mahmood et al., 2019). The electrospun nanofibers consisted of PCL/LEO solutions (R4, R5, R13, R15) had beads increasing with the LEO amount. This may be because LEO does not dissolve in the TFA solvent, as beads are not observed in leo-free PCL solutions. Because normally the addition

of EO reduces the surface tension, as a result, the solvent evaporation rate increases and the bead formation causes weaken. Low surface tension improves nanofiber morphology (Zhang, Yuan, Wu, Han & Sheng, 2005). Callıoglu et al. (2019) produced poly (vinyl pyrrolidone) and gelatin-based polymers containing thyme oil as an active material; and examined them in terms of surface tension, conductivity, etc. According to their study, conductivity and surface tension of the polymers decreased with the concentration of thyme essential oil.

Studies have shown that the increase in viscosity enables the chain structure of the polymer to circulate within each other, therefore, smooth nanofibers without beads will be obtained.

Below are the graphs plotted with shear rate vs shear stress with regression analysis.

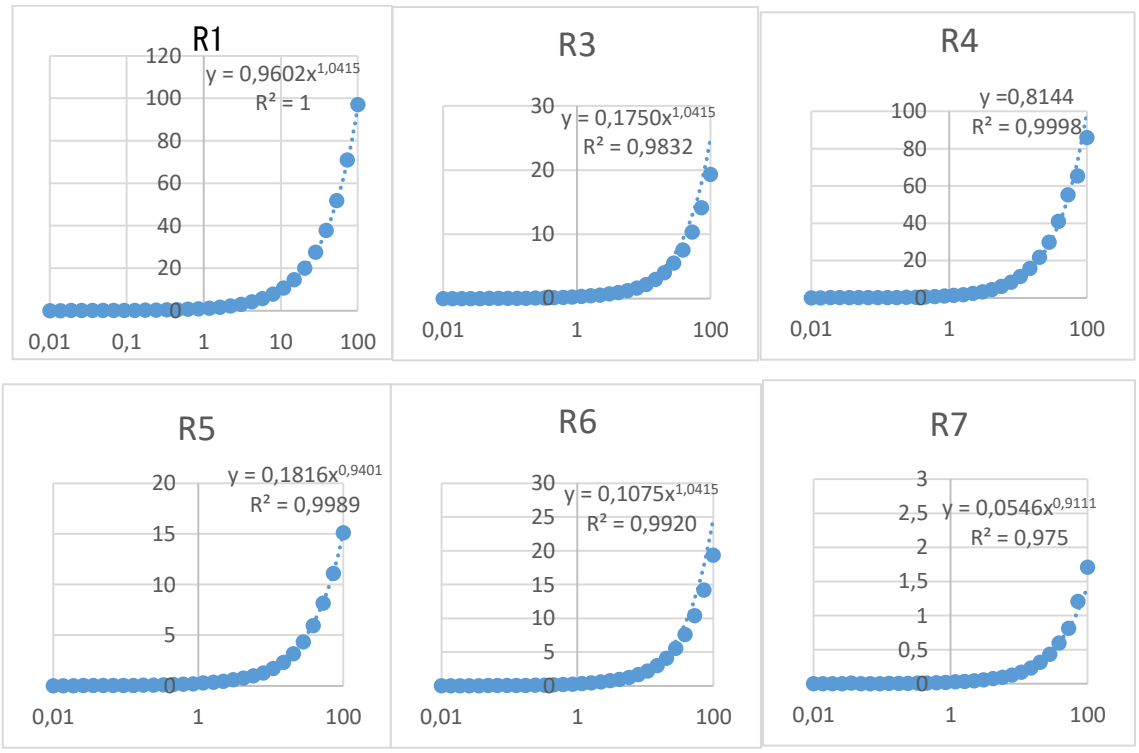

Fig 4.3 Viscosity Values of Polymer Solutions

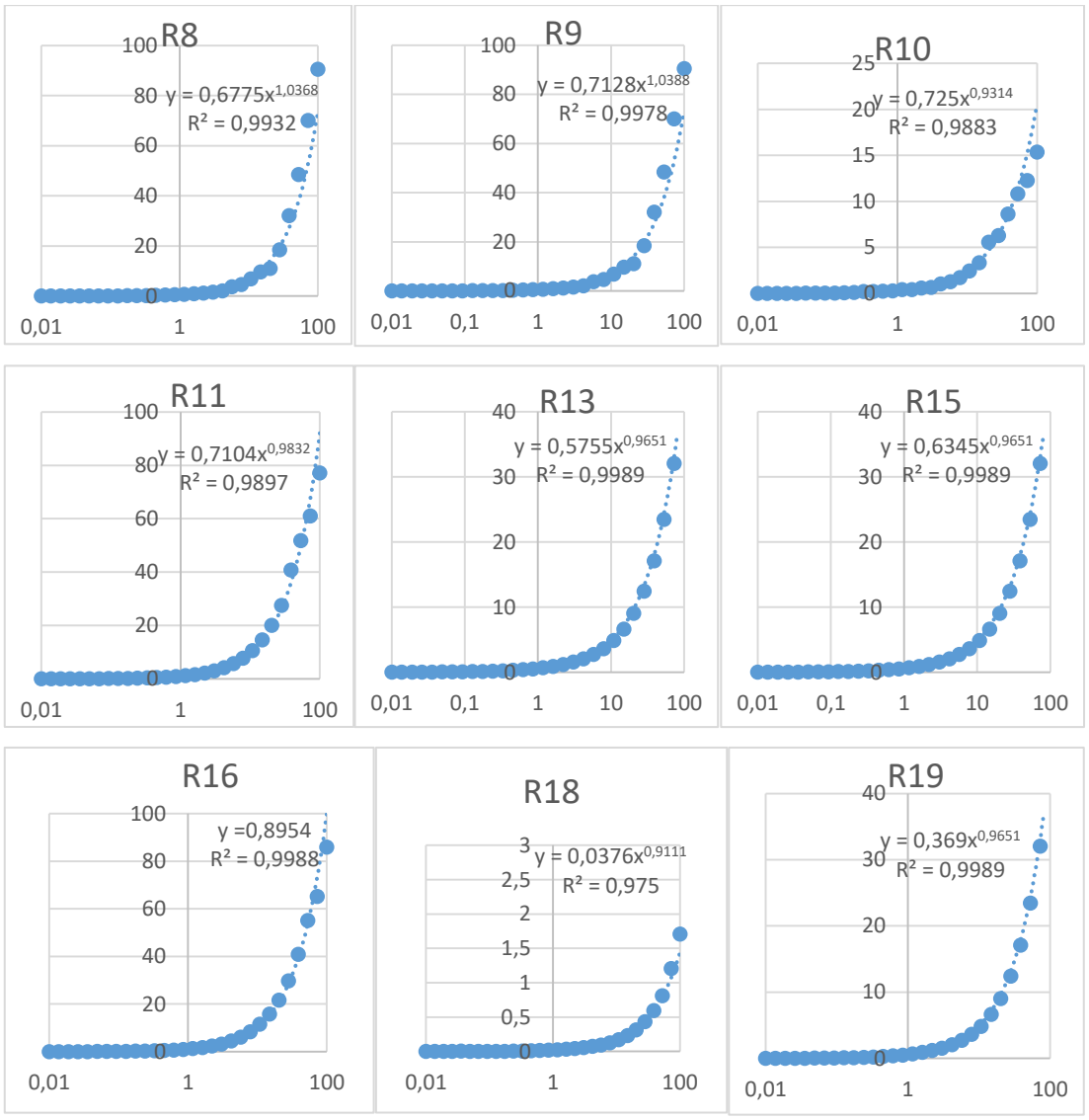

Fig 4.3 Viscosity Values of Polymer Solutions (cont.)

The obtained viscosity values from the graphs were placed in Table 4.3.

Our PCL solutions had much higher viscosity than Gt and Gt/ PCL mix solutions. This is caused by the structural properties of gelatin. It is known that if the viscosity is not high enough for stable jet formation it causes a beaded structure, but this is not the case in our examples. Viscosity decreased with the addition of LEO, resulting in a reduction in nanofiber diameter. Salavic et al., (2019) encapsulated the sage extract with electrospinning and examined its physicochemical and some other properties. According to this study, a large decrease in viscosity was observed with the addition of sage extract. The reason for this may be that the low molecular

weight compounds in the sage extract interact with the polymer chain of the solution.

The dielectric constant of the solutions was measured to understand the polarity of the solution. Charges have a considerably greater impact on a polar solution relative to non-polar ones (Son, Youk, Lee & Park, 2004). In other words, the solutions with the higher dielectric constant are more polar (Isik, Altay & Capanoglu, 2018). There are not many studies on the effect of dielectric constant on electrospinnability and fiber characteristics to the best of our knowledge. The dielectric constant of pure gelatin solution was measured as 13.65 ± 0.13 at 25 °C and there was a decreasing trend by the addition of LEO, as expected. Isik et al. (2018) investigated the effect of dielectric constant on different polymer solutions at 30 MHz and 3 GHz and concluded that the effect of the dielectric constant at 3 GHz was inconclusive and further research is needed. We assume our measurements at 3 GHz will contribute to the literature.

The effects of conductivity, surface tension, dielectric constant and viscosity on average diameter were also investigated. Increased conductivity allows the finer nanofibers (Yu, Williams, Gao, Bligh, Yang & Wang, 2012) like in the samples R10, R11, R18. Although R5 has a low conductivity value, thin nanofiber formation was observed, but bead formation was also observed for this sample and diameters of the beads were not considered. Therefore, we can say that the higher the conductivity value, the lower the diameter of the nanofiber.

For the effect of surface tension, we know that lower surface tension allows uniform and bead-free fibers. For our case, all of the samples were spinnable and uniform. The high dielectric constant prevents the beaded structure and creates a low diameter fiber. In our study, the dielectric constant values of our beaded samples were found to be the lowest. Sample R8, on the other hand, had the lowest dielectric constant value but did not have a beaded structure because the main reason for our samples being beaded was the inability of the TFA solvent to solve the LEO. Even at the lowest viscosity value, all of our solutions were high enough to provide stable jet formation and prevent beaded structure.

Table 4.3 Conductivity, Surface tension and Dielectric constant of the PCL/Gt solutions

Solution	*Conductivity (μS/cm)*	*Surface tension (mN/m)*	*Dielectric constant (ε')*	*Viscosity (mPa)*	*Average diameter (nm)*
R1	6.15 ± 0.05i	23.72±0.03ef	13.11±0.30a	960±13.4a	125±6bcd
R3	290 ± 1g	25.23±0.06cd	9.25±0.04ef	175±7.1g	111±7.7d
R4	6.0 ± 0.07i	23.10±0.03fg	10.31±0.28de	814±8.5b	170±18a
R5	6.75 ± 0.15i	22.85±0.02g	8.37±0.19f	181.5±19g	99±4.2d
R6	344 ± 1e	26.05±0.01b	13.33±0.28a	107±8.5h	115±3.5d
R7	320.5± 0.5f	26.29±0.02b	9.86±0.28de	54±5.6hi	157±6.4ab
R8	508 ± 10c	31.40±0.03a	8.34±0.03f	677±24cd	123±4bcd
R9	156.5 ± 1.5h	24.72±0.03d	13.65±0.03a	712.5±17c	103±7.8d
R10	605.5 ± 5.5a	31.94±0.03a	9.25 ± 0.13ef	72.5±3.5hi	106±1.4abc
R11	605.5 ± 2.5a	31.87±0.03a	10.98±0.31cd	710±14c	112±4.2d
R13	5.5± 0.39i	22.82±0.03fg	12.74±0.33ab	575.5±6.3e	132±14cd
R15	172 ± 0h	24.76±0.03de	9.77±0.01de	634.5±20d	146±15bcd
R16	428.5± 4.5d	26.28±0.03b	11.67±0.06bc	89.5±7.7hi	106±8.4d
R18	545.5± 0.5b	31.51±0.03a	9.05±0.23ef	37±7i	105±4.2d
R19	338.5± 3.5ef	25.71±0.03bc	11.76±0.12b	369±15.6f	112±2.1d

***** *The runs designed in the same proportions by the design expert program were not included in physical properties table (Table 4.3). (R2 is the same as R1; R11 is the same as R12; R14 is the same as R13).*

4.3 Experimental Design

Nineteen separate electrospinning runs were carried out and the antimicrobial activity of the resulting nanofiber mats and the average of the fiber diameters were measured to be used as two responses in the experimental design.

Antimicrobial activities of the nanofibers were calculated as described in 3.11 and to measure the diameters of the produced nanofibers, SEM images of 19 runs were taken and the diameters of 15 random fibers from each run were measured in nanometers and averaged.

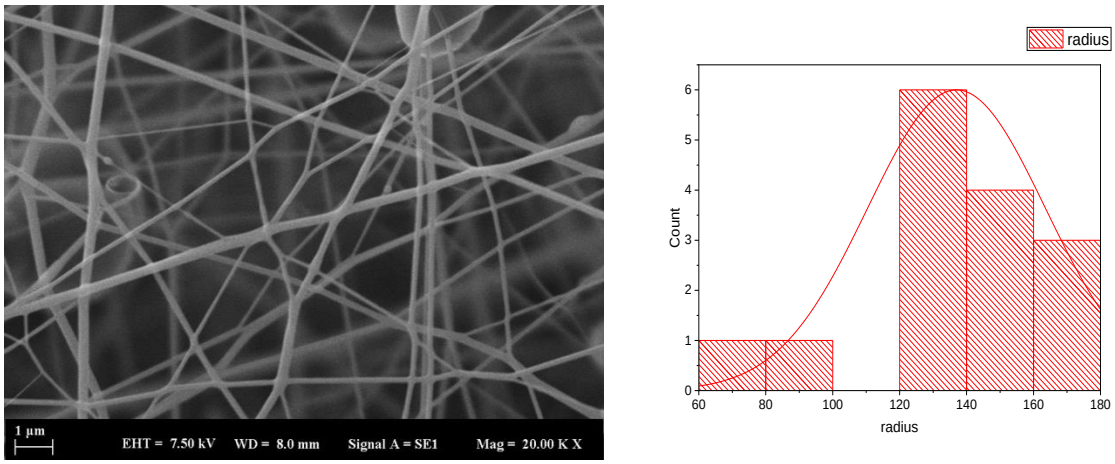

Fig 4.4 PCL nanofibers without LEO (SEM mag. 20000X)

SEM images and the diameter distribution graph of nanofibers containing 10% PCL (w/v) and 0% LEO are seen in Figure 4.4. When the SEM image in the figure was examined, it was observed that the PCL nanofibers had a smooth and beadless morphology. The mean diameter was 129 nm, while the minimum diameter length was 94 and the maximum was 165 nm.

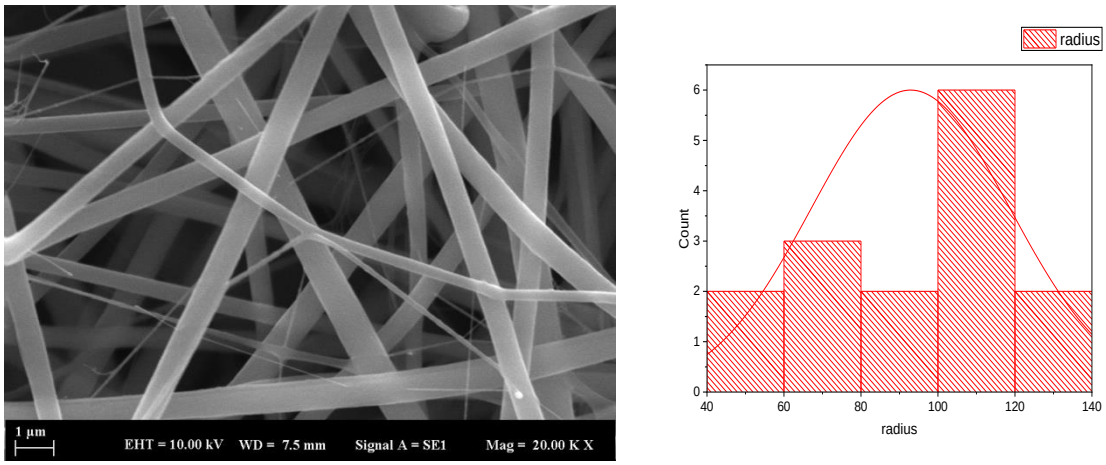

Fig 4.5 PCL/ Gt nanofibers with 5% LEO (SEM mag. 20000X)

SEM images and the diameter distribution graph of nanofibers containing 5% PCL (w/v) and 5% Gt (w/v) with 5% LEO (w/v) are seen in Figure 4.5. When the SEM image in the figure was analyzed, it was observed that the electrospun nanofibers had a smooth and bead-free morphology. The mean diameter was 111 nm, while the minimum diameter length was 56 and the maximum was 179 nm.

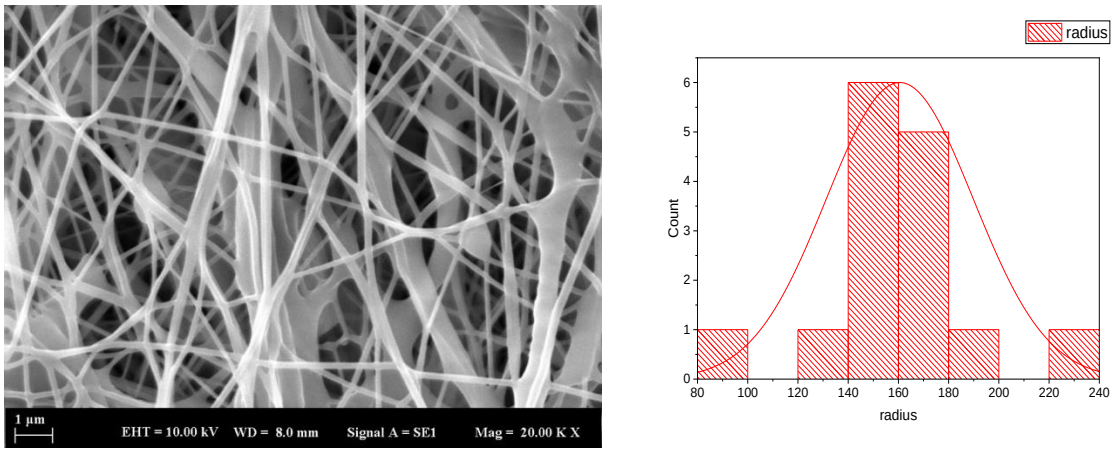

Fig 4.6 PCL nanofibers with 5% LEO (SEM mag. 20000X)

SEM images and the diameter distribution graph of nanofibers containing 10% PCL (w/v) with 5% LEO (w/v) are seen in Figure 4.6. When the SEM image in the figure was analyzed, it was observed that the electrospun nanofibers had some beads between the fibers. The mean diameter was 170 nm, while the minimum diameter length was 95 and the maximum was 217 nm.

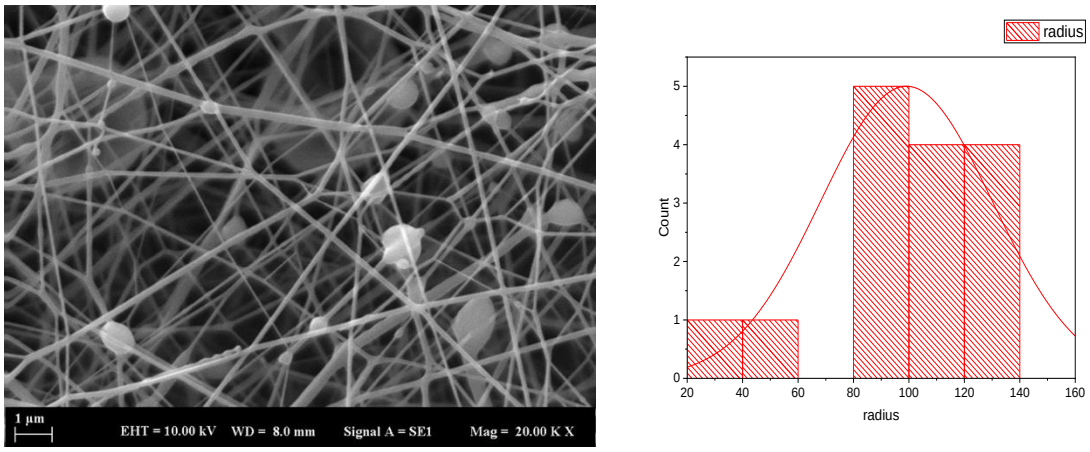

Fig 4.7 PCL nanofibers with 2.5% LEO (SEM mag. 20000X)

SEM images and the diameter distribution graph of nanofibers containing 10% PCL (w/v) with 2.5% LEO (w/v) are seen in Figure 4.7. When the SEM image in the figure was analyzed, it was observed that the nanofibers had very big beads between the thin fibers. The mean diameter was 99 nm (excluding the beads), while the minimum diameter length was 27 and the maximum was 138 nm.

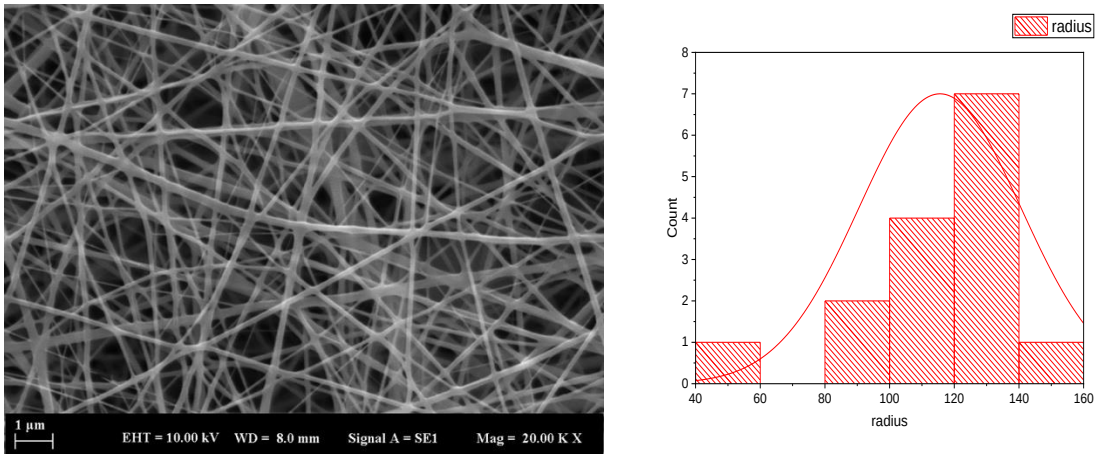

Fig 4.8 PCL/Gt nanofibers with 10% LEO (SEM mag. 20000X)

SEM images and the diameter distribution graph of nanofibers containing 5% PCL (w/v) and 5% Gt (w/v) with 2.5% LEO (w/v) are seen in Figure 4.8. When the SEM image in the figure was examined, it was observed that the nanofibers had smooth, beadless, and thin fiber morphology. The mean diameter was 115 nm, while the minimum diameter length was 45 and the maximum was 154 nm.

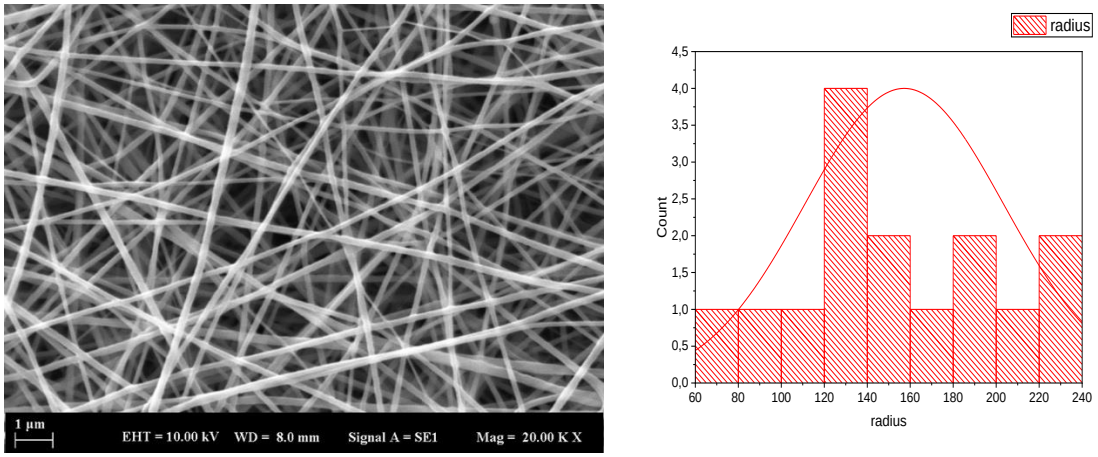

Fig 4.9 PCL/Gt nanofibers with 7.5% LEO (SEM mag. 20000X)

SEM images and the diameter distribution graph of nanofibers containing 2.5% PCL (w/v) and 7.5% Gt (w/v) with 7.5% LEO (w/v) are seen in Figure 4.9. When the SEM image in the figure was examined, it was observed that the nanofibers had smooth, beadles, and thin fibers morphology. The mean diameter was 157 nm, while the minimum diameter length was 79 and the maximum was 226 nm.

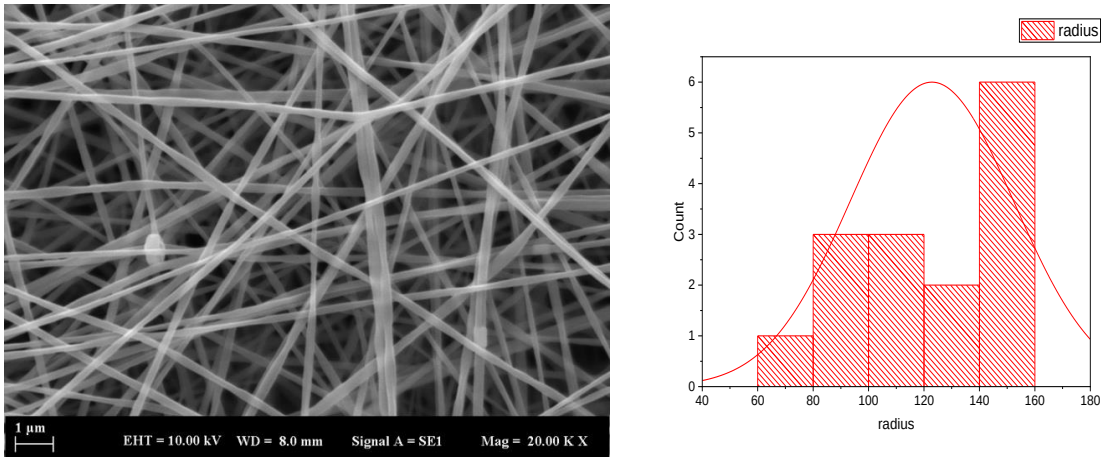

Fig 4.10 Gt nanofibers with 10% LEO (SEM mag. 20000X)

SEM images and the diameter distribution graph of nanofibers containing 10% Gt (w/v) with 10% LEO (w/v) are seen in Figure 4.10. When the SEM image in the figure was examined, it was observed that the nanofibers had one elliptical bead with thin fibers. The mean diameter was 123 nm, while the minimum diameter length was 61 and the maximum was 159 nm.

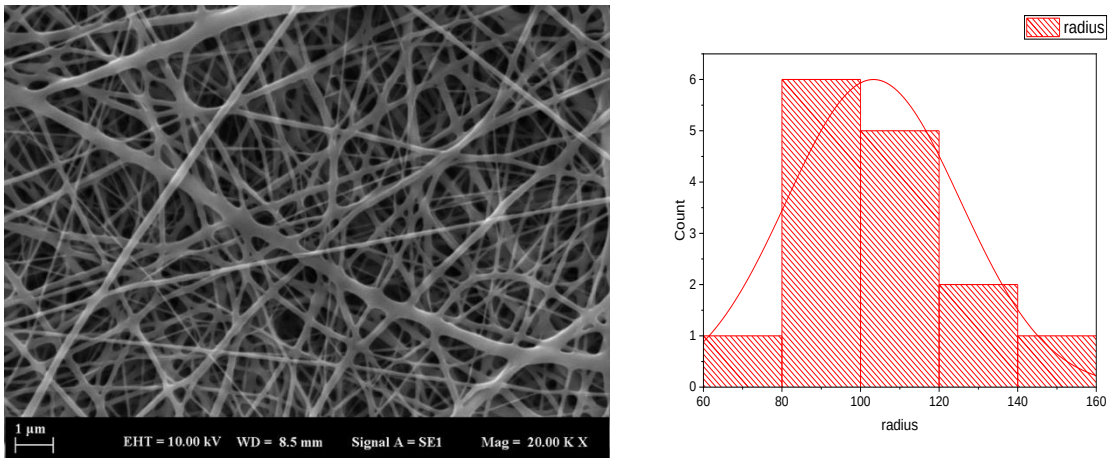

Fig 4.11 PCL/Gt nanofibers with 7.5% LEO (SEM mag. 20000X)

SEM images and the diameter distribution graph of nanofibers containing 7.5% Gt (w/v) and 2.5% Gt (w/v) with 7.5% LEO (w/v) are seen in Figure 4.11. When the SEM image in the figure was examined, it was observed that the nanofibers had smooth and bead-free morphology. The mean diameter was 103 nm, while the minimum diameter length was 69 and the maximum was 149 nm.

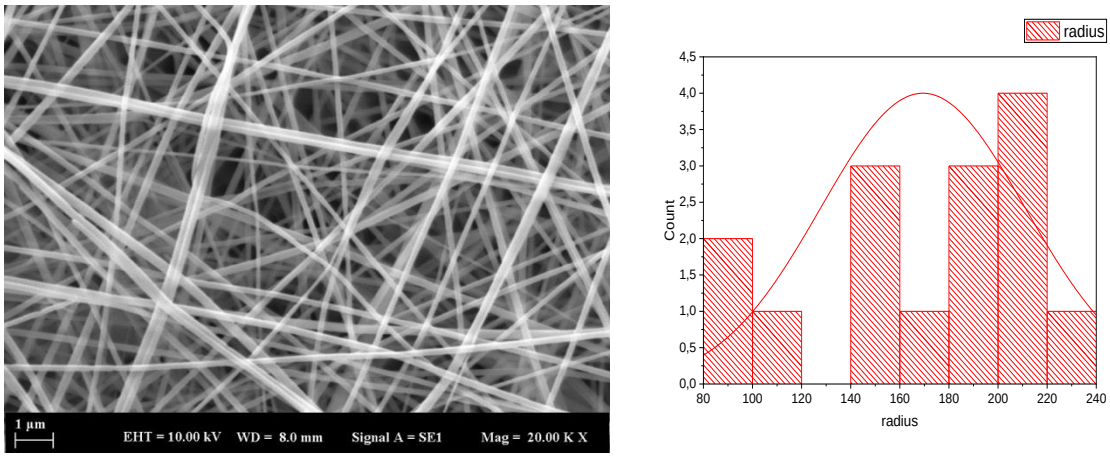

Fig 4.12 Gt nanofibers with 5% LEO (SEM mag. 20000X)

SEM images and the diameter distribution graph of nanofibers containing 10% Gt (w/v) with 5% LEO (w/v) are seen in Figure 4.12. When the SEM image in the figure was examined, it was observed that the nanofibers had smooth, bead-free and homogenous morphology. The mean diameter was 169 nm, while the minimum diameter length was 90 and the maximum was 221 nm.

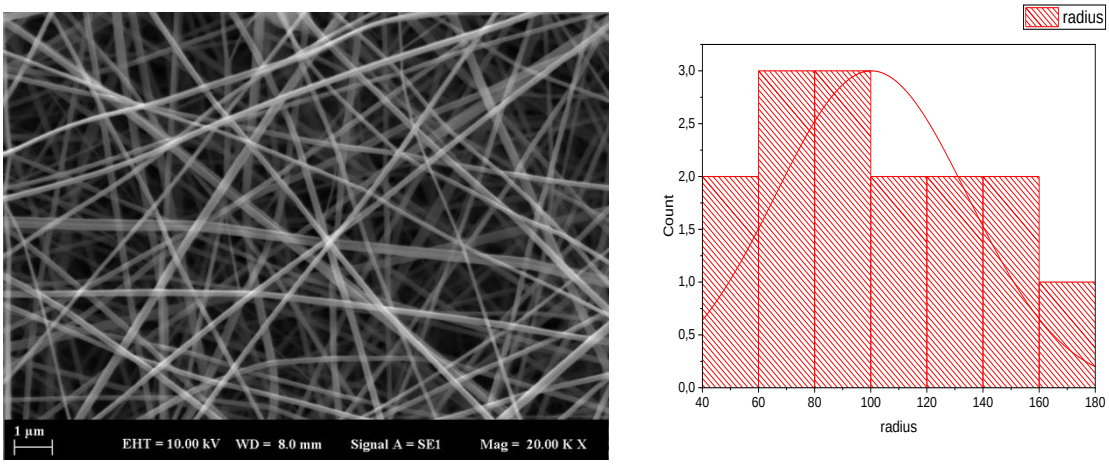

Fig 4.13 Gt nanofibers with 0% LEO (SEM mag. 20000X)

SEM images and the diameter distribution graph of nanofibers containing 10% Gt (w/v) without LEO are seen in figure 4.13. When the SEM image in the figure was examined, it was observed that the nanofibers had smooth, bead-free and homogenous morphology. The mean diameter was 100 nm, while the minimum diameter length was 46 and the maximum was 163 nm.

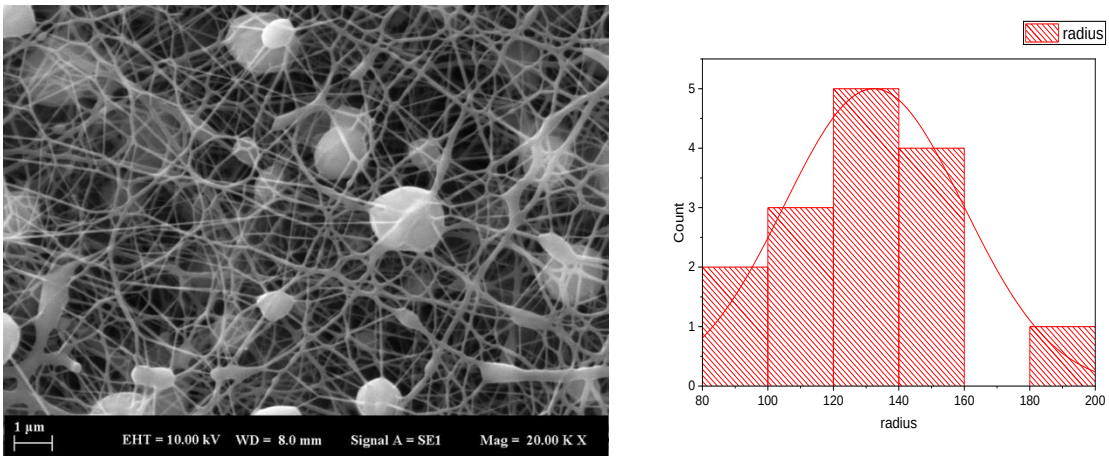

Fig 4.14 PCL nanofibers with 10% LEO (SEM mag. 20000X)

SEM images and the diameter distribution graph of nanofibers containing 10% PCL (w/v) with 10% LEO (w/v) are seen in figure 4.14. When the SEM image in the figure was analyzed, it was observed that the nanofibers had very big beads between the thin fibers. The mean diameter was 132 nm (excluding the beads), while the minimum diameter length was 90 and the maximum was 196 nm.

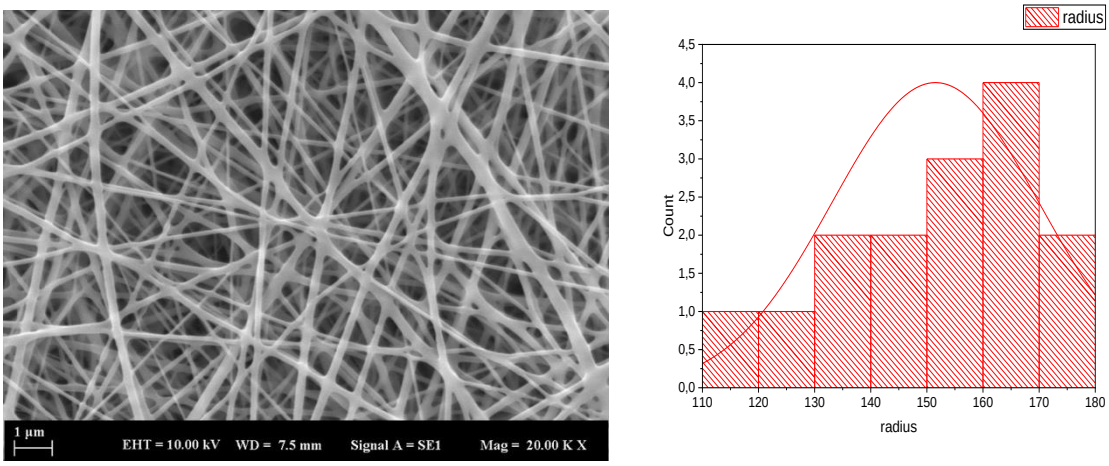

Fig 4.15 PCL/ Gt nanofibers with 2.5% LEO (SEM mag. 20000X)

SEM images and the diameter distribution graph of nanofibers containing 7.5% PCL (w/v), 2.5% Gt (w/v) and 2.5% LEO (w/v) are seen in figure 4.15. When the SEM image in the figure was examined, it was observed that the nanofibers had smooth and bead-free morphology. The mean diameter was 151 nm, while the minimum diameter length was 114 and the maximum was 177 nm.

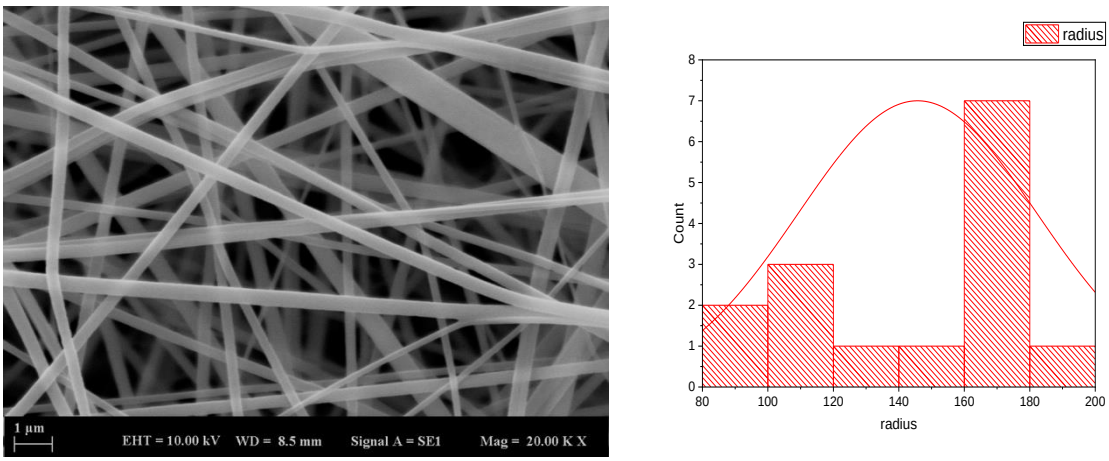

Fig 4.16 PCL/ Gt nanofibers with 2.5% LEO (SEM mag. 20000X)

SEM images and the diameter distribution graph of nanofibers containing 2.5% PCL (w/v), 7.5% Gt (w/v) and 2.5% LEO (w/v) are seen in figure 4.16. When the SEM image in the figure was examined, it was observed that the nanofibers had smooth and bead-free morphology. The mean diameter was 146 nm, while the minimum diameter length was 88 and the maximum was 190 nm.

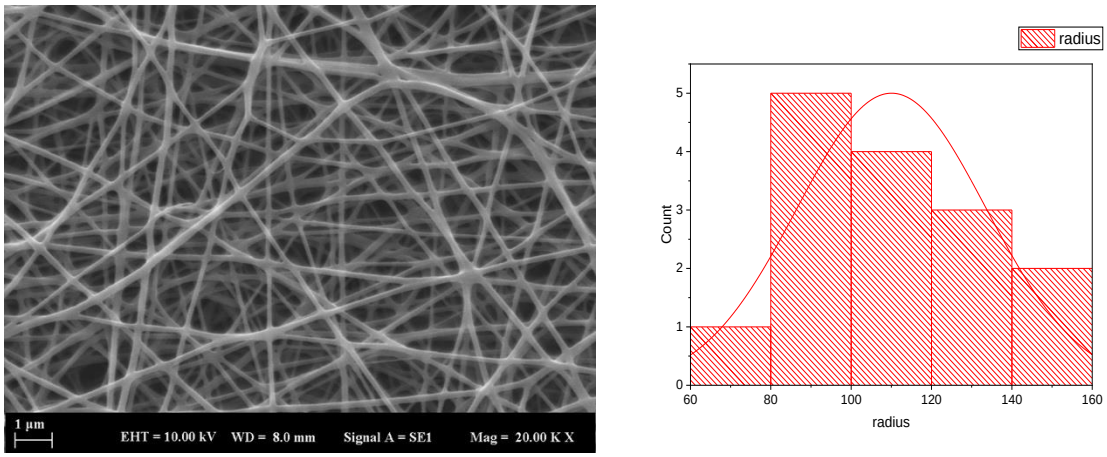

Fig 4.17 Gt nanofibers with 10% LEO (SEM mag. 20000X)

SEM images and the diameter distribution graph of nanofibers containing 10% Gt (w/v) and 10% LEO (w/v) are seen in figure 4.17. When the SEM image in the figure was examined, it was observed that the nanofibers had smooth, bead-free and homogenous morphology. The mean diameter was 110 nm, while the minimum diameter length was 69 and the maximum was 154 nm.

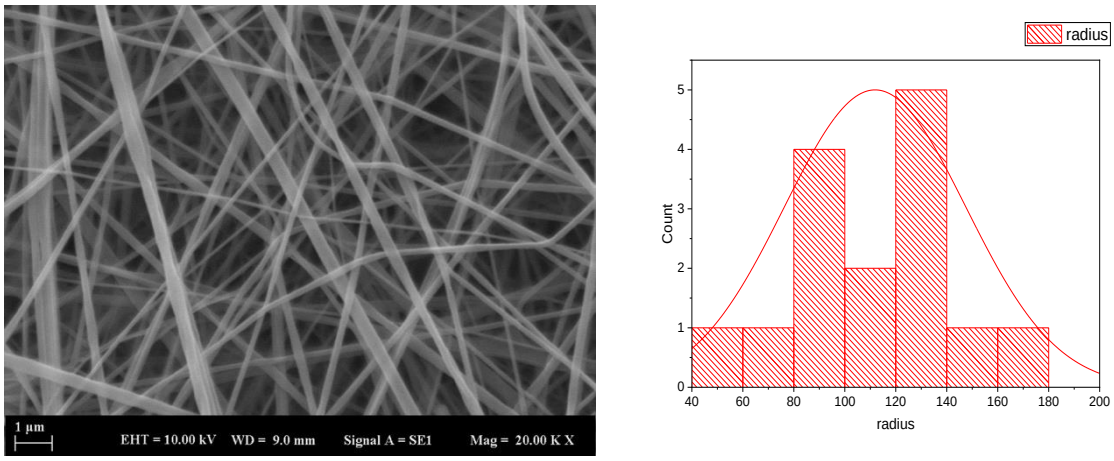

Fig 4.18 Gt nanofibers with 0% LEO (SEM mag. 20000X)

SEM images and the diameter distribution graph of nanofibers containing 5% PCL (w/v) and %5 Gt (w/v) without LEO are seen in figure 4.18. When the SEM image in the figure was examined, it was observed that the nanofibers had smooth and bead-free morphology. The mean diameter was 112 nm, while the minimum diameter length was 54 and the maximum was 180 nm.

Table 4.4 Experimental design with response values

Std	*Run*	*Block*	*PCL*	*Gelatin*	*Factor*	*R1*	*R2*
18	1	Block 1	1.00	0.00	0.00	129	0
5	2	Block 1	1.00	0.00	0.00	120	0
1	3	Block 1	0.50	0.50	0.50	111	98
7	4	Block 1	1.00	0.00	0.50	170	97.5
14	5	Block 1	1.00	0.00	0.25	99	95
19	6	Block 1	0.50	0.50	1.00	115	99.3
13	7	Block 1	0.25	0.75	0.75	157	99
15	8	Block 1	0.00	1.00	1.00	123	99
11	9	Block 1	0.75	0.25	0.75	103	98.5
2	10	Block 1	0.00	1.00	0.50	169	97
16	11	Block 1	0.00	1.00	0.00	100	0
8	12	Block 1	0.00	1.00	0.00	132	0
6	13	Block 1	1.00	0.00	1.00	148	99.1
17	14	Block 1	1.00	0.00	1.00	151	99
10	15	Block 1	0.75	0.25	0.25	146	93.8
12	16	Block 1	0.25	0.75	0.25	106	92
4	17	Block 1	0.50	0.50	1.00	118	99
9	18	Block 1	0.00	1.00	1.00	110	99.2
3	19	Block 1	0.50	0.50	0.00	112	0

The diameters of nanofibers composed of different ratios of Gt, PCL and LEO were measured and averaged for the Response 1. Antimicrobial activities of the nanofibers were calculated as described in section 3.11 for the Response 2 value.

Table 4.5 Constraints for the Experimental Design

Name	Goal	Lower Limit	Upper Limit	Lower Weight	Upper Weight	Importance
PCL	is in range	0.000	1.00	1.00	1.00	3
Gt	is in range	0.000	1.00	1.00	1.00	3
LEO	is in range	0.000	1.00	1.00	1.00	3
R1	minimize	100.	290.	1.00	1.00	3
R2	maximize	0.000	99.3	1.00	1.00	4

Solution

Number	PCL	Gt	LEO	R1	R2	Desirability	
1	0.602	0.398	0.950	115.	99.3	0.966	Selected
2	1.00	0.000	0.982	120.	99.3	0.954	
3	0.000	1.00	0.990	131.	99.3	0.927	

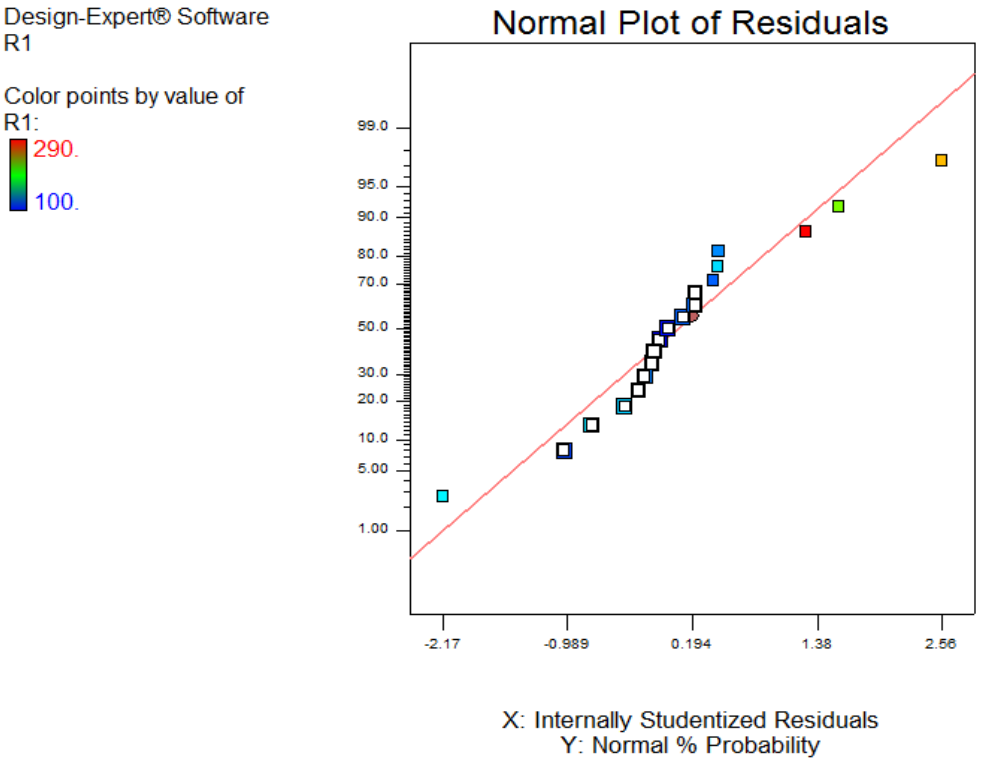

Fig 4.19 Normal Plot of Residuals for R1

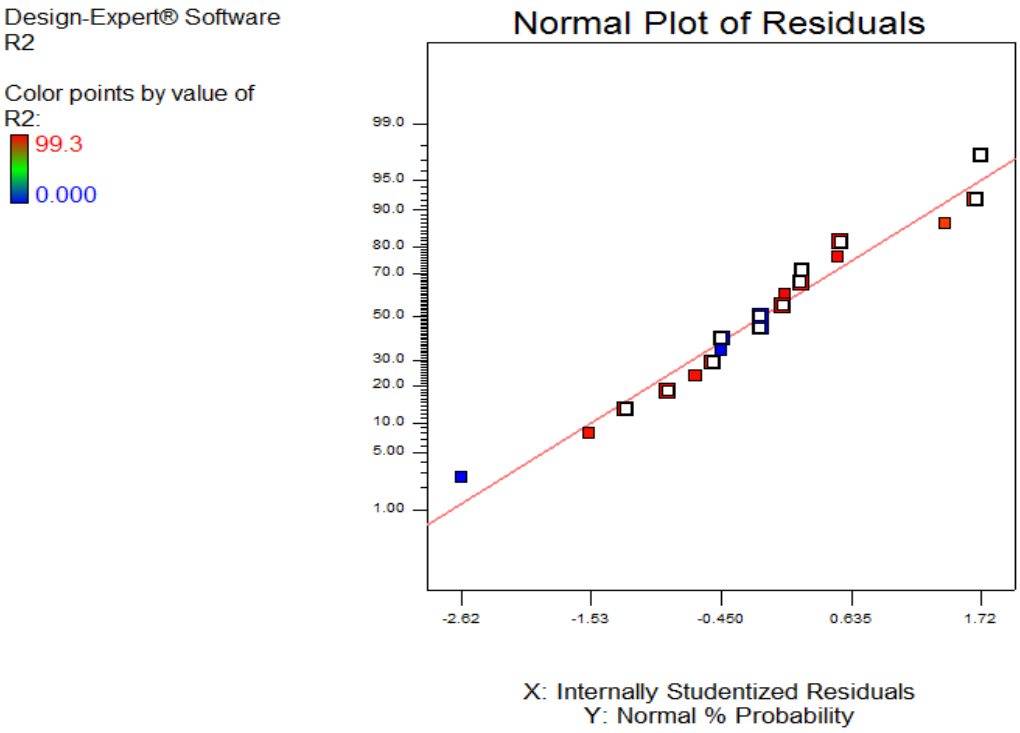

Fig 4.20 Normal Plot of Residuals for R2

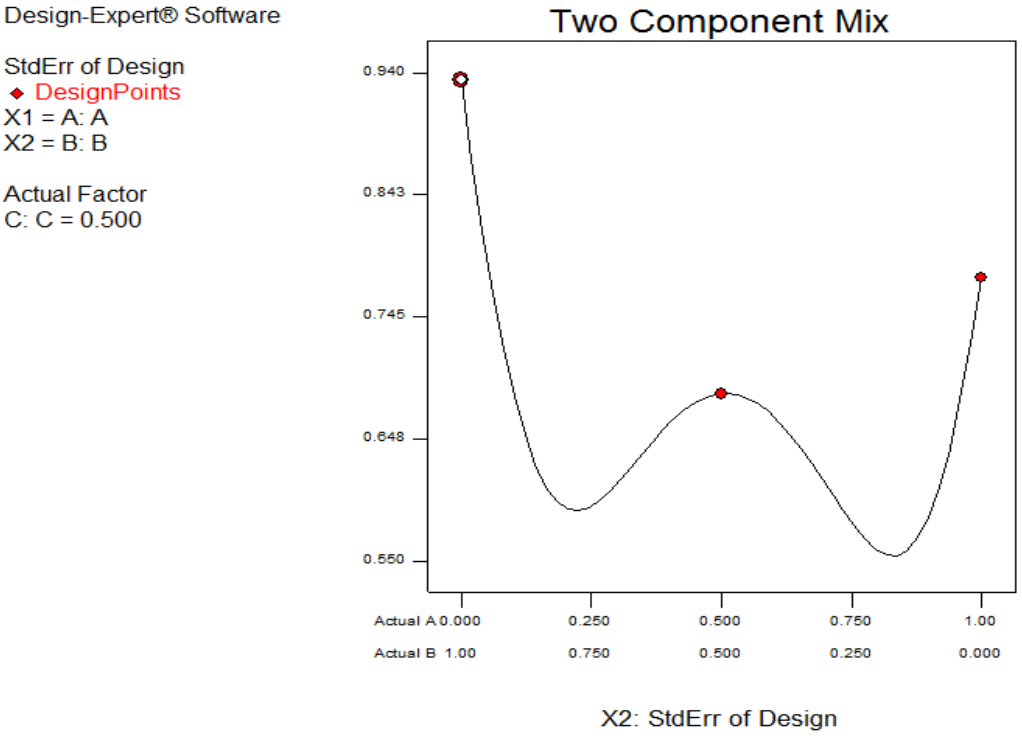

Fig 4.21 Standard Error of Design

All subsequent analyzes were performed using the optimum PCL / Gt nanofiber determined in the experimental design. In addition, fibers consisting only of gelatin incorporated LEO (0, 5, 10%) have also been investigated as they can be used as edible packaging material.

4.4 FTIR Analysis of Nanofiber Scaffolds

The FTIR spectra of Gt nanofiber scaffolds and LEO are shown in Fig 4.22 and 4.23. The potential interactions between the components of the Gt fibers and LEO were detected by FTIR-ATR. Electrospun fibers were collected, dried for 24 h before analysis. The broadband at 1640 cm^{-1} is due to C = O stretching vibration (amide-I) spectrum and the band at 1537 cm^{-1} shows the N-H deformation for the amide II in the gelatin film spectrum (Wu, San, Guo, Ge & Zhang, 2017).

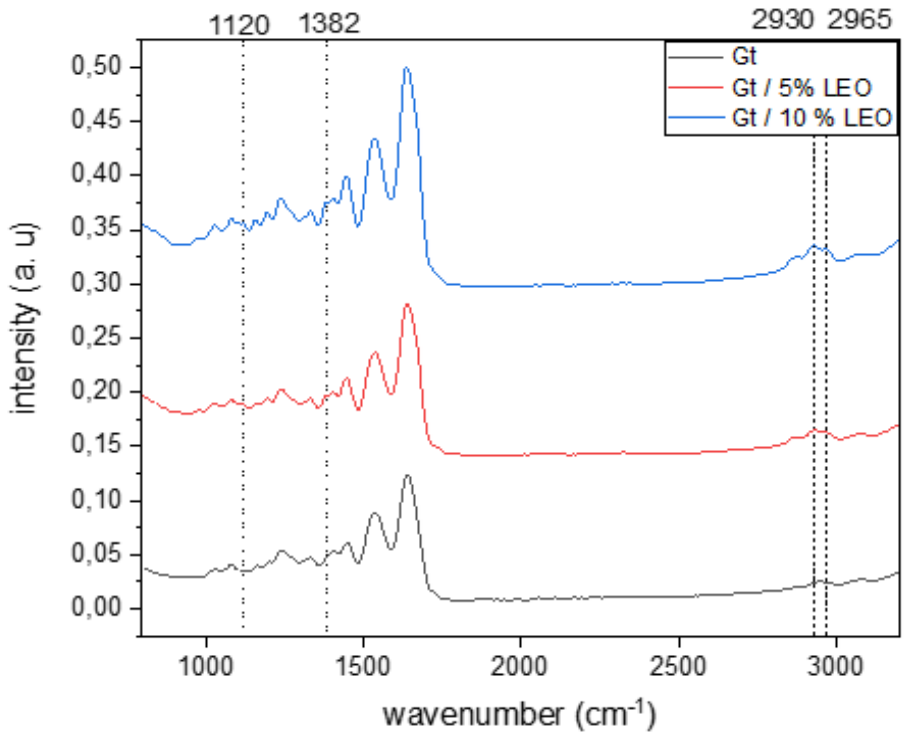

Fig 4.22 ATR-FTIR spectrum of 0, 5, and 10% lemongrass oil embedded Gt nanofibers

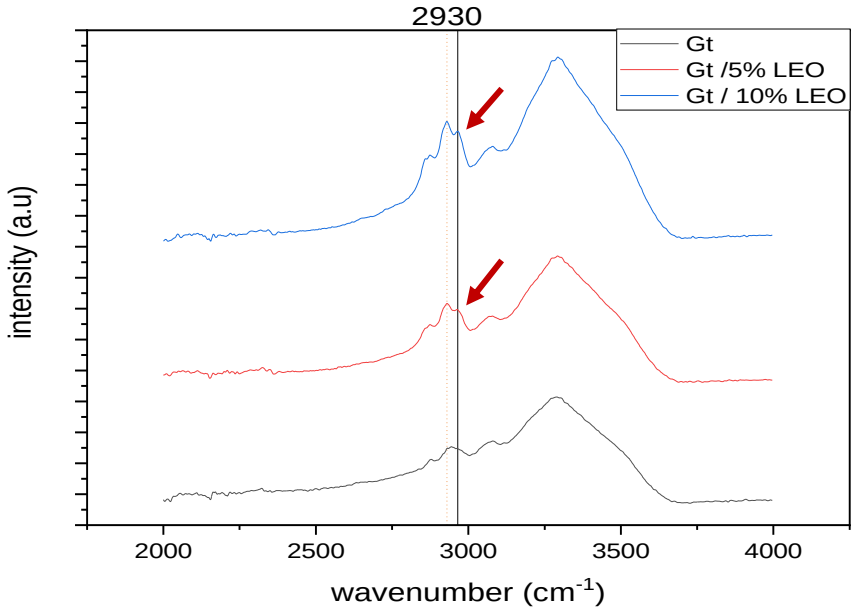

Fig 4.22* ATR-FTIR spectrum of 0, 5, and 10% lemongrass oil embedded Gt nanofibers (*between 2000-4000 cm^{-1} wavenumbers)

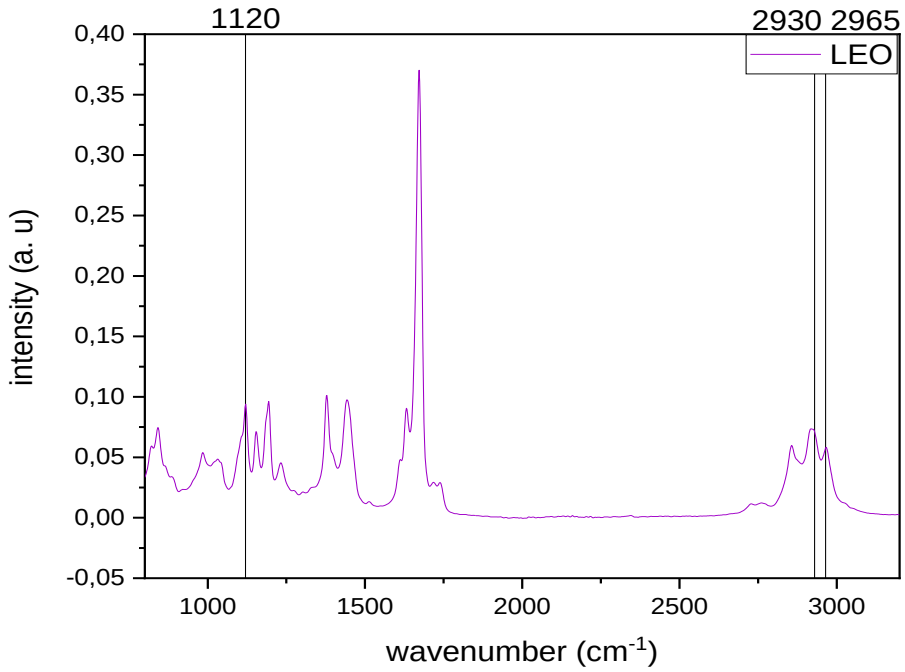

Fig 4.23 ATR-FTIR spectrum of lemongrass essential oil (LEO)

As a feature of axial deformation vibrations of the C-H bond in aliphatic molecules, the three bands were observed at 2965, 2930, and 2866 cm^{-1} in the spectrum of LEO. The absorption peak detected at 1672 cm^{-1} is aligned with the axial vibration of C = O bond of unsaturated α, β-aldehydes, which relates to the geranial and neral conjugate structure. The medium strength bands are identical to the CH_3 bonds at 1443 and 1378 cm^{-1}.

The bonds between 1193 and 1120 cm^{-1} are associated with the C – O bonds of carboxylic acids and alcohols of some minor compounds in the LEO (Antonioli, Fontanella & Echeverrigaray, 2020). Some of these characteristic LEO peaks, shown by straight dot lines in Figure 4.23, were observed in Gt / LEO nanofibers, although they were not found in pure Gt nanofibers. In the polymeric matrix, the existence of these peaks is a confirmation of LEO being in the structure. These results comply with the data already published in the literature (Vafania et al., 2019). The enhancement of the peak of LEO embedded gelatin nanofibers at 2930 cm^{-1} was due to hydrophobicity increase by the addition of LEO. Comparable findings were obtained by Silvia Garcia et al. (2020) who encapsulated essential oils in chitosan microparticles against Candida albicans biofilms. Overall, the Gt/LEO films displayed characteristic LEO and Gt peaks, and there were no additional peaks indicating effective encapsulation with only physical interactions.

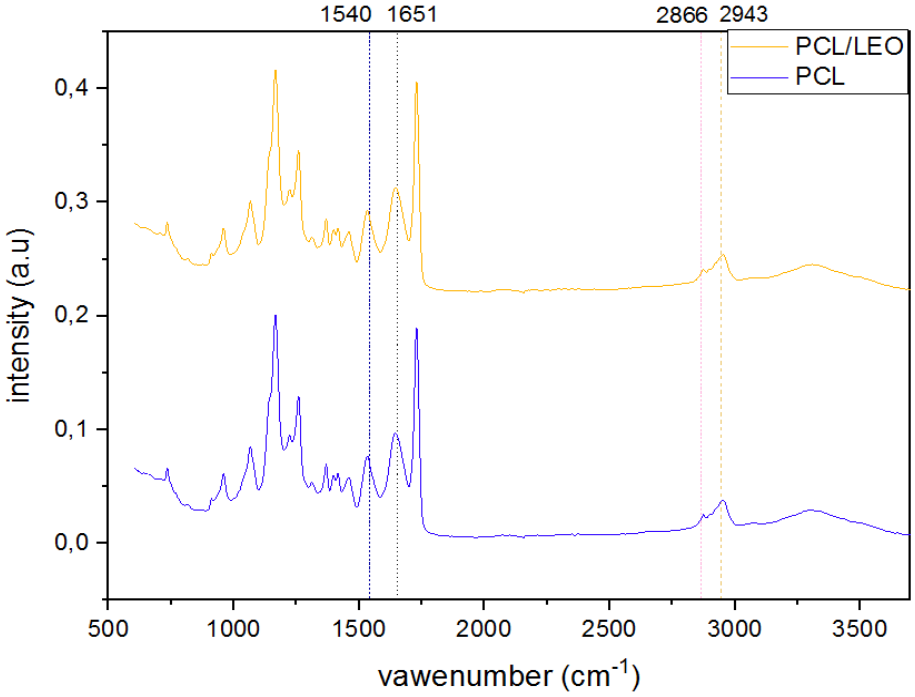

Fig 4.24 ATR-FTIR spectrum of PCL/Gt and PCL/Gt/LEO nanofibers

In Fig 4.24, some characteristic peaks of PCL are seen at 2939 cm^{-1} (asymmetric CH_2 stretching), 2868 cm^{-1} (symmetric CH_2 stretching), 1729 cm^{-1} (ester carbonyl stretching), 1294 cm^{-1} (C-O and C-C stretching), 1239 cm^{-1} (asymmetric COC stretching). Some protein bands that can be associated with both random coil and α-helix conformation of gelatin are observed at 1640 cm^{-1} (amide I) and 1537 cm^{-1} (amide II) with PCL characteristic peaks. FTIR spectra of PCL/Gt nanofibers exhibited both characteristic peaks of PCL and Gt which is a confirmation of existence of these polymers without chemical interaction. In addition to these characteristic peaks, LEO integrated PCL/Gt nanofibers, also showed certain LEO specific peaks which confirms a successful physical blend. Ren et al. (2017), evaluated PCL/gelatin composite nanofiber structures and performed FTIR analysis. They found that some of the bands they observed in the PCL/Gt mixture belong to gelatin and some to PCL, therefore the successful hybrid polymer production with FTIR. Kuppan et al. (2013), also worked on PCL/Gt scaffolds characterization and found out that PCL/Gt nanofibers exhibited protein bands at 1651 cm^{-1} and 1551 cm^{-1} which was attributed to (amide I) and (amide II), respectively similar to our study.

4.5 DSC Analysis of Nanofibers

Differential Scanning Calorimetry (DSC) analysis was used to evaluate the thermal stability of the Gt & Gt / LEO and PCL/Gt & PCL/Gt/LEO nanofibers. Thermal profiles of unloaded and LEO loaded gelatin nanofibers are depicted in Fig 4.25. Gt nanofibers displayed an endothermic peak at around 93°C while LEO loaded nanofibers showed the peak at slightly increased temperatures in direct proportion to LEO amount (Fig 4.23). Gelatin is a material that can be easily denatured due to its collagen content involving the breakup of the triple-helix structure by breaking hydrogen bonds and rearranging the triple-helix into a random configuration, under decent conditions, such as a gelling phase, the chains will undergo a transformation from a conformational disorder to recover the triple-helix structure. (Zhang, Venugopal, Huang, Lim & Ramakrishna, 2006). Thus, the distinctive endothermic peaks mostly referred to denaturation temperature (Td). The denaturation temperature for pure gelatin was 93 °C, for 5% LEO incorporated Gt nanofibers was 102 °C, and for 10% LEO/Gt nanofibers was 112°C. Denaturation temperature of Gt nanofibers containing EO was higher than the pure Gt fibers. This may be because EO improves the relationship between water and Gt, hence increase the water retention capacity. The enthalpy associated with this peak reflects the energy needed for hydrogen bond rupture, covalent bond destruction, and interactions with van der Waals. Contrastingly, EO functions as a plasticizer and improves the mobility of molecular gelatin chains, contributing to the decrease of enthalpy denaturation that leads to the decrease of denaturation enthalpy. However, it may also interfere with chains of polypeptides and raise enthalpy denaturation. This can be due to the reaction of the hydrophobic gelatin chain with the essential oil alkyl groups and benzene ring, where essential oil is a guest molecule within the Gt or Gt chains (Tavassoli-Kafrani, Goli & Fathi, 2018).

Feyzioglu and Tornuk (2016) observed that the melting temperature of chitosan nanoparticles increased slightly with the addition of EOs. DSC data can also be used as an indicator of encapsulation performance. If there is a strong interaction between the active substance and the encapsulating polymer, no characteristic peaks belonging to the encapsulated active material are noticed (Feyzioglu &

Tornuk, 2016). DSC thermograms of 3 samples are very similar and characteristic peaks were not observed, which proved the partial or total encapsulation of LEO in the gelatin nanofibers was occurred.

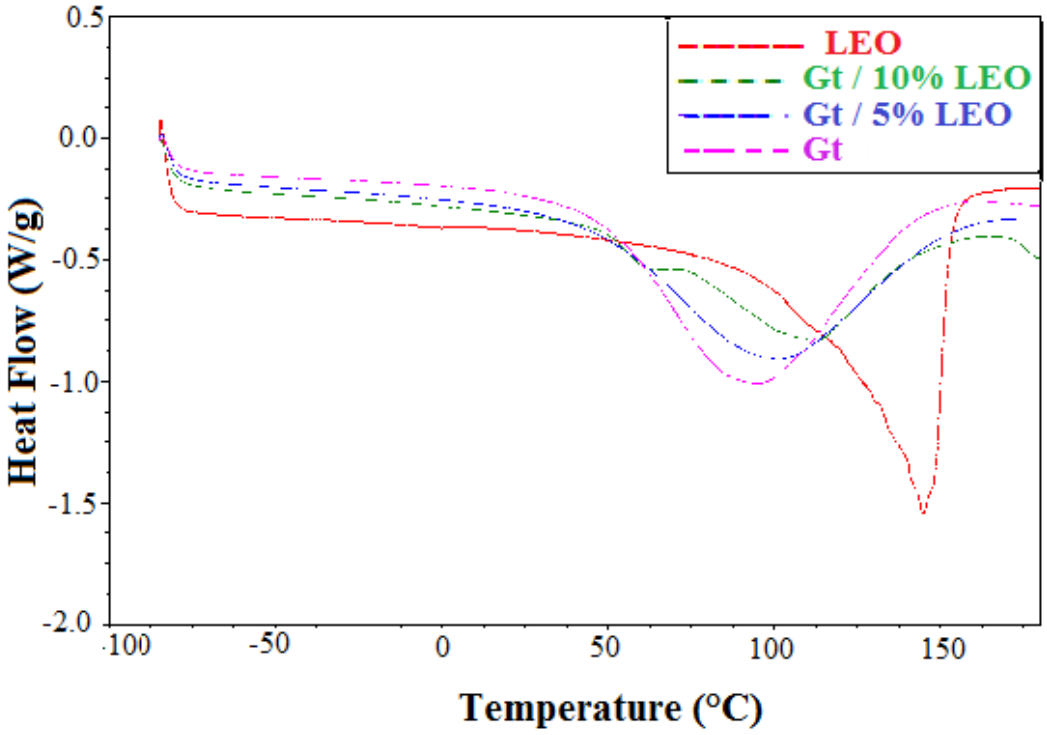

Fig 4.26 DSC Thermogram of LEO and Gt/ LEO nanofibers

In order to increase the heat retention capacity and water repellency of electro-spun fibers, crosslinking materials can be used for the purpose. Chen et al. (2009) cross to composite structure composed of polyethylene glycol and cellulose acetate by adding binder material, in order to improve both thermal stability and water repellency properties.

Thermal profiles of unloaded and LEO loaded optimum PCL/Gt/LEO nanofibers are shown in Fig 4.27. Two major endothermic peaks are seen in the Fig 4.24 represent the melting temperature of PCL and Gt. The first sharp peak is around 52 °C for PCL/Gt and, 50 °C for PCL/Gt/LEO samples are the melting temperature of PCL (T_m). The second sharp peak for PCL/Gt nanofibers was at 87.5°C which represent the melting point of Gt. The peak at 111°C is related with melting point of PCL/Gt/LEO

nanofibers. When fibers contain LEO, there is a slight shift at the melting temperature due interaction of LEO with carbonyl groups on PCL chains. The experiment conducted until 230 °C where third endothermic peaks started which would indicate the thermal decomposition (T_d) of the polymers.

Fallah et al. curcumin encapsulated into PCL/Gt mix. They found out in their DSC thermograms that the melting temperature was 100°C for Gt. This peak is due to the loss of water from gelatin nanofibers and PCL melted at 60°C.

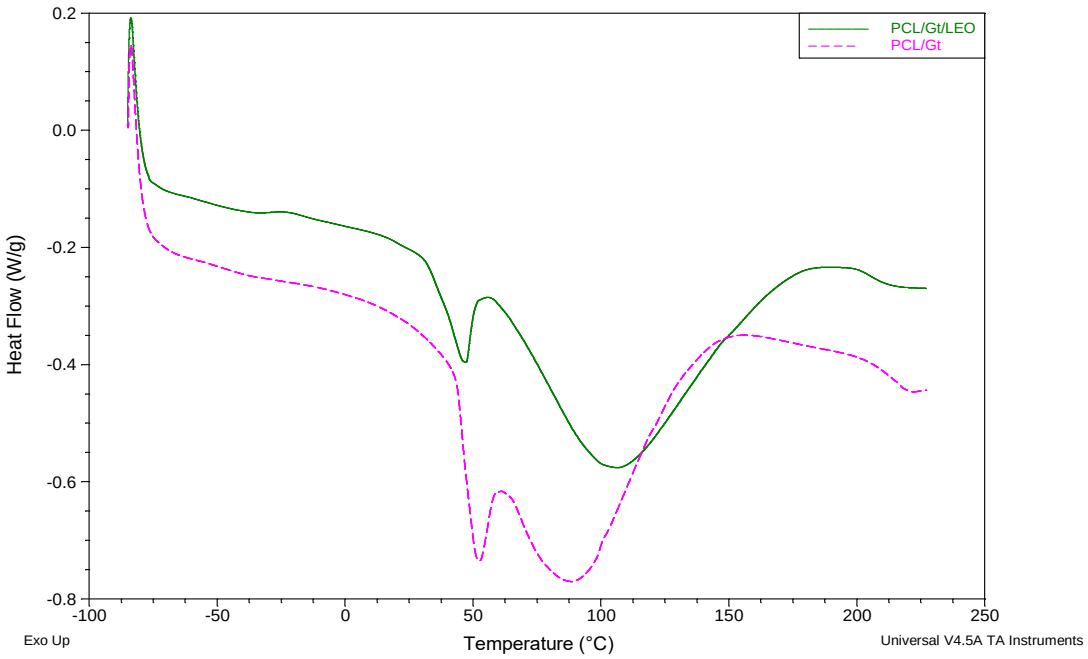

Fig 4.27 DSC Thermogram of PCL/ Gt/ LEO nanofibers

4.6 In vitro Antibacterial Activity of Nanofibers

The primary cause for food spoilage and the causative agent of food-borne diseases is the growth of spoilage or pathogenic microorganisms. Therefore, antimicrobial activity is one of the most desired functions in the food packaging field. Fig 4.28 demonstrates the antimicrobial efficiency of LEO embedded gelatin nanofibers against *S.* Typhimurium and *S. aureus* as common food-borne disease bacteria. Unloaded nanofilms showed no antimicrobial effect against two selected bacteria.

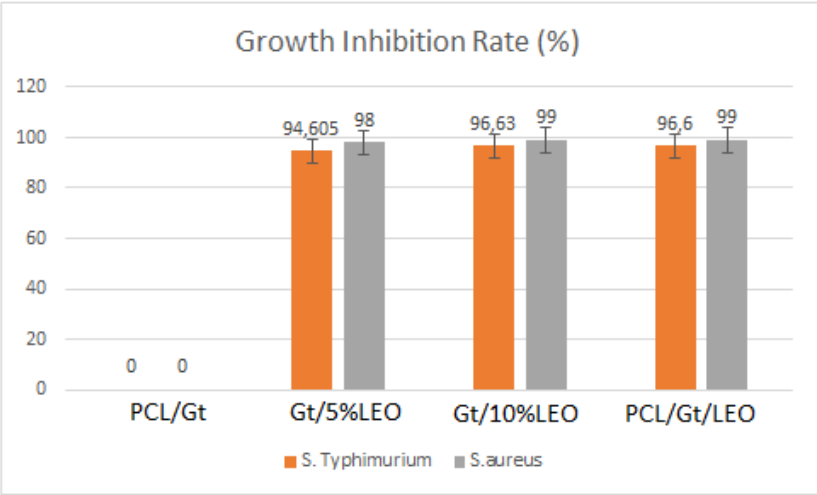

Fig 4.28 Growth Inhibition Rate of Gt and Gt/PCL nanofibers

The antimicrobial effect of 10% LEO / Gt film was better than 5% LEO / Gt film against both bacteria, as predicted. 10% LEO / Gt film exhibited 99.09% inhibition rate against *S. aureus* bacteria, though having slightly less effect against *S.* Typhimurium (96.63%). Gt/PCL nanofibers also showed as much antimicrobial activity as 10% LEO/Gt nanofibers. 98.55% inhibition rate were observed against *S. aureus* bacteria. Increased antibacterial activity of nanofibers for *S. aureus* rather than *S.* Typhimurium may be due to the gram properties of the bacteria. Gram-negative bacteria are more antibiotic-resistant than gram-positive bacteria due to the composition differences of their cell wall (Breijyeh, Jubeh & Karaman, 2020). Antibacterial activity of EOs encapsulated coatings against Gram-positive bacteria has been reported to be significantly higher than that of Gram-negative bacteria in literature by several researchers such as Amalraj et al. (2020) and Noori et al. (2018). In contrast, Tang et al. (2019) evaluated peppermint and chamomile essential oil embedded gelatin nanofibers against *S. aureus* and *E. coli* and found that the EO/nanofibers showed better antibacterial activity against Gram-negative bacteria. Our results suggested that LEO embedded gelatin and PCL/Gt nanofibers may have a place on active food packaging field with high antimicrobial activity.

4.7 Application Study

4.7.1 Determination of Physicochemical Properties of Chicken Samples During 7-Days Storage

Physicochemical properties and the changes of the PCL/Gt/LEO coated chicken samples were monitored in this part of the study. The change in pH, color and *Salmonella* load was measured to assess the quality change in chicken samples over 7 days.

4.7.1.1 Color

Color is important parameter for both as an indicator of freshness and as a factor that affects the preference of the consumer. Meat color change during storage and retail is inevitable, and therefore strategies to extend color stability make a significant contribution to profitability. The most important of these strategies is active packaging (Suman & Joseph, 2013).

L* (lightness) values of control and PCL/Gt/LEO nanofibers coated chicken samples are shown in the Table 4.6. A high value of L* means that the chicken samples have a brighter color. Although there is a decrease in the L* value of control and packaged chicken samples during storage, the rate of decrease in control is higher. Except for the L* value increase observed in packaged chicken on day 1 of storage, L* values decreased in all samples during storage. There was no significant difference ($p>0.05$) between the control and packaged samples on days 0 and 3rd for the L* values. At the end of the 7 days, we can conclude that unpackaged chicken samples were darker than LEO encapsulated nanofibers coated chickens.

Konuk Takma and Korel evaluated effect of black curcumin encapsulated active packaging on chicken breasts during storage. They reported that L* values of the samples decreased by storage and darker colored chickens were obtained at the end of the storage.

Table 4.6. L* values of chicken breast samples during seven days of storage

	Storage time (days)				
	0	***1***	***3***	***5***	***7***
Control	50.95 ± 0.83a	48.63 ± 0.71a	44.75 ± 1.50a	43.25 ± 0.62a	43.03 ± 1.05a
Packaged	52.35 ± 0.14a	53.11 ± 0.96b	49.18 ± 0.65a	48.60 ± 0.22b	47.54 ± 0.73b

*Columns having different letters are significantly different ($p \leq 0.05$).

The change during seven days storage in a* (redness) values of control and packaged chicken samples are shown in table 4.10. While the all a* values of the control chicken samples increased, the a* value of the packaged chicken samples decreased on the 3rd and 7th days. The significant difference ($p < 0.05$) between the a* values of the packaged and unpackaged samples occurred on the 3rd day of the storage and continued until the last day. The change in a* values of the packaged samples, on the 1st day of storage was insignificant due to the very short contact time and the short interaction time of essential oil compounds with chicken samples. Lin et al. evaluated effect of oregano essential oil encapsulated nanofibers on chicken samples during storage and observed that a* values were decreased by time in the agreement of our study.

Table 4.7. a* values of chicken breast samples during seven days of storage

	Storage time (days)				
	0	***1***	***3***	***5***	***7***
Control	1.74 ± 0.01a	1.86 ± 0.03a	1.96 ± 0.04a	2.24 ± 0.12a	2.55 ± 0.07a
Packaged	1.62 ± 0.02a	1.72 ± 0.01a	1.56 ± 0.05b	1.61 ± 0.03b	1.37 ± 0.02b

*Columns having different letters are significantly different ($p \leq 0.05$).

The change during seven days storage in b* (yellowness) values of control and packaged chicken samples are shown in table 4.11. 0 and 1st day of the storage there was no significant difference ($p > 0.05$) between the samples. Although the b* values

of the control and packaged chicken samples increased every day, a statistically significant increase ($p>0.05$) was not observed on the first day. The difference in b* values between the packaged chicken and control after the 3rd day was found to be significant ($p<0.05$). Zhang et al. found that the b* values of samples treated with rosemary and thyme essential oil increased during storage.

Table 4.8. b* values of chicken breast samples during seven days of storage

	Storage time (days)				
	0	***1***	***3***	***5***	***7***
Control	6.76 ± 0.08a	7.15 ± 0.05a	8.87 ± 0.03a	9.08 ± 0.03a	10.19 ± 0.01a
Packaged	6.89 ± 0.01a	6.99 ± 0.01a	7.68 ± 0.18b	8.03 ± 0.02b	8.52 ± 0.27b

*Columns having different letters are significantly different ($p\leq0.05$).

Total color difference (ΔE) values of control and PCL/ Gt /LEO nanofibers coated chicken pieces are shown in table 4.12. During the storage, total color difference values were increased for both packaged and control samples. There was significant difference ($p<0.05$) between the total color difference values of control and packaged samples at the day 7. First, third and fifth days of storage there was not statistical difference between the ΔE values. The highest color change was observed at the seventh day for control samples.

Noori et al. evaluated the antimicrobial effect of ginger oil based edible food packaging on chicken samples. Color measurements were made to determine the quality characteristics thus, ΔE values were measured during storage. The change in ΔE values of the coatings containing ginger essential oil increased during storage, but this increase was less than the control sample. GEO addition increased the ΔE values of coated sample The highest ΔE was noted for control sample at day 8 as 6.96.

Table 4.9. ΔE values of chicken breast samples during seven days of storage

	Storage time (days)				
	0	***1***	***3***	***5***	***7***
Control	-	1.99 ± 0.11a	3.41±0.53a	5.81± 0.79a	7.76±0.50a
Packaged	-	2.29 ± 0.25a	3.27±0.14a	3.83±0.10a	6.52±0.76b

*Columns having different letters are significantly different (p≤0.05).

4.7.1.2 pH

pH values of control and PCL/ Gt /LEO nanofibers coated chicken breast samples are monitored during the storage. At the day 0, the pH value found as 5.99. The amount of glycogen in meat affects the pH value. The first pH value of chicken varies depending on factors such as slaughter time, type of chicken, slaughter method, feed type, transportation time, etc. pH value of packaged chicken samples decreases until the 5th day of the storage while the pH of control samples was increasing gradually. The final pH value at the 7th day was 5.75 for control and 6.83 for the packaged chicken samples.

In their research, Giatrakou et al. investigated the impact of chitosan and thyme oil on a ready-to-cook chicken product. During storage, the pH of the control sample was observed to increase, but the pH of the sample coated with thyme oil fluctuated and gradually returned to its original pH (Giatrakou, Ntzimani & Savvaidis, 2010).

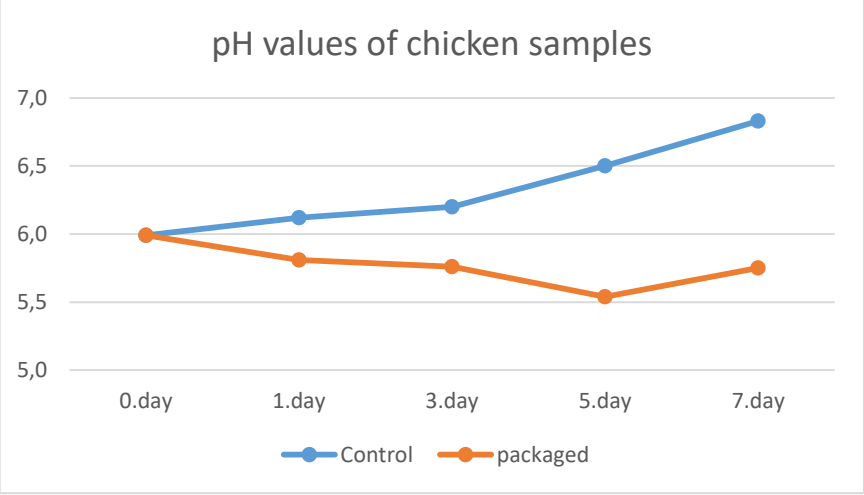

Fig 4.29 pH values of chicken samples during the 7-days storage

4.7.2 Determination of Microbiological Properties of Chicken Breasts During 7-days Storage

Chicken meat is a frequent cause of foodborne poisoning and is a good carrier of *Salmonella. Salmonella* is a zoonotic pathogen that negatively affects human health and also causes economic losses. *Salmonella* is transmitted during slaughter, from slaughter tools, air, workers, etc to poultry. Active packaging systems are used as an alternative solution to ensure food safety in chicken meat and to prevent *Salmonella* growth. (Abd El-Aziz, 2013).

Control and LEO encapsulated PCL/Gt nanofibers coated chicken samples monitored during the seven days storage, microbiologically. *Salmonella* Typhimurium load change is given in the table 4.12.

Salmonella load of the control chicken samples increased from 6.19 $\pm$ 0.11 CFU/g to 6.97 $\pm$ 0.34 CFU/g during one week of storage. The microbial load of packaged chicken samples decreased over 5 days, but increased slightly on day 7. *Salmonella* load, which was 6.24 $\pm$ 0.30 CFU/g at the beginning, decreased to 4.77 $\pm$ 0.27 CFU/g at the end of the 7th day. 1.47 CFU/g microbial reduction was achieved. There was no statistical difference ($p>0.05$) between control and packaged chicken samples on day 1 of storage. From the 3rd day of storage, a statistically significant difference ($p<0.05$) in microbial load was observed between the control and packaged chickens.

Table 4.10. *Salmonella* Typhimurium load of chicken breast samples during seven days of storage (CFU/g)

	Storage time (days)				
	0	***1***	***3***	***5***	***7***
Control	6.19 ± 0.11a	6.41± 0.26a	6.64± 0.12a	6.89 ± 0.22a	6.97± 0.34a
Packaged	6.24 ± 0.30a	6.17 ± 0.15a	5.87± 0.10b	4.73 ± 0.55b	4.77 ± 0.27b

*Columns having different letters are significantly different ($p\leq0.05$).

Soysal et al. evaluated antimicrobial active packaging against on physicochemical and microbial properties of chicken drumsticks. They incorporated antimicrobial substances such as nisin, chitosan into low density polyethylene (LDPE) and coated chicken drumsticks. At the end of the 6th day storage, they achieved maximum 1 log reduction of microbial load (Soysal et al., 2015).

Shahbazi et al. assessed the application of basil essential oil to control *Listeria monocytogenes* in chicken meatballs to extend shelf life. *Listeria* amount decreased 2.66 log at the end of storage. The basil essential oil contains small amounts of lipophilic compounds such as a-pinene and terpinene, which destroy the integrity of the cell membrane and disrupt cytoplasmic cell membrane function. This high decontamination rate has been associated with a synergistic effect with the essential oil's main components with these minor compounds (Shahbazi, Karami & Shavisi, 2018).

Ahmed et al. investigated the antimicrobial properties of cinnamon oil incorporated film against *L. monocytogenes* and *S.* Typhimurium in chicken samples with and without high pressure treatment. They stored packaged chicken samples for 20 days at 4 °C and full inactivation of PLA/PEG/CIN films for test microorganisms, especially for L. monocytogenes could not be achieved. However, when the packaging applied in combination with HP treatment, samples were successfully stored for 26 days (Ahmad, Hiremath, & Jacob 2016).

4.8 Conclusions

The lemongrass essential oil showed good antimicrobial efficiency against both gram-negative (*S.* Typhimurium, *E. coli)* and gram-positive (*S. aureus, B. cereus)* bacteria when tested by disc diffusion method, MIC, and MBC. According to GC-MS analysis results, citral and Z-citral were the main constituents of the LEO. Electrospinnability of the polymer solution was investigated by measuring conductivity, surface tension, and dielectric constant. SEM results showed that we achieved the produce smooth, cylindrical, and bead-free nanofibers. Both 10% and 5% LEO embedded nanofibers showed strong antimicrobial activity against both

gram-negative and positive bacteria. FTIR analysis results implied that there was a successful penetration of LEO into gelatin fibers and the thermal analyses showed that polymeric encapsulation matrices improve the thermal stability of LEO. The application study showed that fabricated PCL/Gt/LEO nanofibers help prolonging the shelf life of chicken samples. It also helped preserve the color and pH value of chickens. 1.47 CFU/g microbial reduction was achieved during the seven days storage period. The findings of this study indicate that PCL/Gt/LEO nanofibers have a high potential for application as active food packaging.

The first hypothesis tested in this thesis was that electrospinning is an efficient method for the manufacture of antimicrobial food packaging material. Lemongrass oil (LEO) is an effective antimicrobial agent that can be used for this purpose. The second one was coating chicken breast samples with lemongrass oil encapsulated nanofibers would reduce the microbial load and prolong the shelf life of chicken breasts. Moreover, some objectives are tested. According to our results LEO has been found to show antimicrobial activity against some microorganisms that cause foodborne illnesses.

It was observed that lemongrass oil did not dissolve with TFA and caused a beaded structure and the other parameters required for nanofiber production with optimum properties were examined. Accordingly, it was determined that as the concentration of essential oils increased, the viscosity of the prepared solution decreased and its electrical conductivity decreased. FTIR spectroscopy indicated successful encapsulation by showing the peaks of LEO in LEO encapsulated nanofibers. The growth of *Salmonella* in nanofibers coated chicken meat samples was controlled. In addition, color and pH change has slowed compared to unpackaged samples. The following suggestions can be drawn from this study: Study can be expanded with various essential oils other than lemongrass oil. Also, other food products can be tested for microbiologically and physiochemically. Its effect for other microorganisms such as molds can also be investigated.

5
References

Abd El-Aziz, D. M. (2013). Detection of Salmonella typhimurium in retail chicken meat and chicken giblets. *Asian Pacific journal of tropical biomedicine*, 3(9), 678-681.

Ahmed, J., Hiremath, N., & Jacob, H. (2016). Efficacy of antimicrobial properties of polylactide/cinnamon oil film with and without high-pressure treatment against Listeria monocytogenes and Salmonella typhimurium inoculated in chicken sample. *Food Packaging and Shelf Life,* 10, 72-78.

Alharbi, A. R., Alarifi, I. M., Khan, W. S., & Asmatulu, R. (2016). Highly hydrophilic electrospun polyacrylonitrile/polyvinypyrrolidone nanofibers incorporated with gentamicin as filter medium for dam water and wastewater treatment. *Journal of Membrane and Separation Technology*, 5(2), 38-56.

Amalraj, A., Haponiuk, J. T., Thomas, S., & Gopi, S. (2020). Preparation, characterization and antimicrobial activity of polyvinyl alcohol/gum arabic/chitosan composite films incorporated with black pepper essential oil and ginger essential oil. *International journal of biological macromolecules,* 151, 366-375.

Antonioli, G., Fontanella, G., Echeverrigaray, S., Delamare, A. P. L., Pauletti, G. F., & Barcellos, T. (2020). Poly (lactic acid) nanocapsules containing lemongrass essential oil for postharvest decay control: In vitro and in vivo evaluation against phytopathogenic fungi. *Food Chemistry,* 326, 126997.

Anu Bhushani, J., & Anandharamakrishnan, C. (2014). Electrospinning and electrospraying techniques: Potential food based applications. In *Trends in Food Science and Technology* (Vol. 38, Issue 1, pp. 21–33). Elsevier Ltd. https://doi.org/10.1016/j.tifs.2014.03.004

El Asbahani, A., Miladi, K., Badri, W., Sala, M., Addi, E. A., Casabianca, H., ... & Elaissari, A. (2015). Essential oils: from extraction to encapsulation. *International journal*

of pharmaceutics, 483(1-2), 220-243.

Aytac, Z., Ipek, S., Durgun, E., Tekinay, T., & Uyar, T. (2017). Antibacterial electrospun zein nanofibrous web encapsulating thymol/cyclodextrin-inclusion complex for food packaging. *Food Chemistry*, *233*, 117–124.

Bhardwaj, N., & Kundu, S. C. (2010). Electrospinning: a fascinating fiber fabrication technique. *Biotechnology advances,* 28(3), 325-347.https://doi.org/10.1016/j.foodchem.2017.04.095

Breijyeh, Z., Jubeh, B., & Karaman, R. (2020). Resistance of Gram-negative bacteria to current antibacterial agents and approaches to resolve it. Molecules, 25(6), 1340.

Burt S. (2004). Essential oils: their antibacterial properties and potential applications in foods--a review. *International journal of food microbiology,* 94(3), 223–253. https://doi.org/10.1016/j.ijfoodmicro.2004.03.022

Callıoglu, F. C., Güler, H. K., & Çetin, E. S. (2019). Emulsion electrospinning of bicomponent poly (vinyl pyrrolidone)/gelatin nanofibers with thyme essential oil. *Materials Research Express,* 6(12), 125013.

Can, F. O., Demirci, A., Puri, V. M., & Gourama, H. (2014). Decontamination of hard cheeses by pulsed UV light. *Journal of food protection,* 77(10), 1723-1731.

Chen, C., Wang, L. ve Huang, Y. (2009). Crosslinking of the electrospun

polyethylene glycol/cellulose acetate composite fibers as shape-stabilized phase

change materials. *Materials Letters,* 63, 569-571.

Desai, K. G. H., & Park, H. J. (2005). Recent developments in microencapsulation of food ingredients. *Drying Technology*. https://doi.org/10.1081/DRT-200063478

Echegoyen, Y., Fabra, M. J., Castro-Mayorga, J. L., Cherpinski, A., & Lagaron, J. M. (2017). High throughput electro-hydrodynamic processing in food encapsulation and food packaging applications. *Trends in Food Science & Technology,* 60, 71-79.

Elzein, Na Elzein, T., Nasser-Eddine, M., Delaite, C., Bistac, S., & Dumas, P. (2004). FTIR study of polycaprolactone chain organization at interfaces. *Journal of colloid and interface science*, 273(2), 381-387.

Fathi, M., Martín, Á., & McClements, D. J. (2014, September 1). Nanoencapsulation of food ingredients using carbohydrate based delivery systems. *Trends in Food Science and Technology*. Elsevier Ltd. https://doi.org/10.1016/j.tifs.2014.06.007

Feyzioglu, G. C., & Tornuk, F. (2016). Development of chitosan nanoparticles loaded with summer savory (Satureja hortensis L.) essential oil for antimicrobial and antioxidant delivery applications. LWT, 70, 104-110.

Fonseca, L. M., Radünz, M., dos Santos Hackbart, H. C., da Silva, F. T., Camargo, T. M., Bruni, G. P., ... & Dias, A. R. (2020). Electrospun potato starch nanofibers for thyme essential oil encapsulation: antioxidant activity and thermal resistance. *Journal of the Science of Food and Agriculture,* 100(11), 4263-4271.

García-Moreno, P. J., Stephansen, K., van der Kruijs, J., Guadix, A., Guadix, E. M., Chronakis, I. S., & Jacobsen, C. (2016). Encapsulation of fish oil in nanofibers by emulsion electrospinning: Physical characterization and oxidative stability. *Journal of food engineering,* 183, 39-49.

Ghorani, B., & Tucker, N. (2015). Fundamentals of electrospinning as a novel delivery vehicle for bioactive compounds in food nanotechnology. *Food Hydrocolloids,* 51, 227-240.

Giatrakou, V., Ntzimani, A., & Savvaidis, I. N. (2010). Effect of chitosan and thyme oil on a ready to cook chicken product. *Food microbiology,* 27(1), 132-136.

Gibbs, B. F., Kermasha, S., Alli, I., & Mulligan, C. N. (1999). Encapsulation in the food industry: A review. *International Journal of Food Sciences and Nutrition*, *50*(3), 213–224. https://doi.org/10.1080/096374899101256

Han Lyn, F., & Nur Hanani, Z. A. (2020). Effect of Lemongrass (Cymbopogon citratus) Essential Oil on the Properties of Chitosan Films for Active Packaging. *Journal of Packaging Technology and Research*, *4*(1), 33–44. https://doi.org/10.1007/s41783-019-00081-w

Hanani, Z. N., Roos, Y. H., & Kerry, J. P. (2014). Use and application of gelatin as potential biodegradable packaging materials for food products. *International journal of biological macromolecules,* 71, 94-102.

Hasanpour Ardekani-Zadeh, A., & Hosseini, S. F. (2019). Electrospun essential oil-doped chitosan/poly(ε-caprolactone) hybrid nanofibrous mats for antimicrobial food biopackaging exploits. *Carbohydrate Polymers*, *223*(July), 115108. https://doi.org/10.1016/j.carbpol.2019.11510

Isik, B. S., Altay, F., & Capanoglu, E. (2018). The uniaxial and coaxial encapsulations of sour cherry (Prunus cerasus L.) concentrate by electrospinning and their in vitro bioaccessibility. Food chemistry, 265, 260-273.

Jumepaeng, T., Prachakool, S., Luthria, D. L., & Chanthai, S. (2013). Determination of antioxidant capacity and α-amylase inhibitory activity of the essential oils from citronella grass and lemongrass. *International Food Research Journal*.

King, A. H. (1995). Encapsulation of food ingredients: a review of available technology, focusing on hydrocolloids.

Koç, M., Sakin, M., & Kaymak Ertekin, F. (2010). Microencapsulation and its Applications in Food Technology. Pamukkale University Journal of Engineering Sciences, 16(1), 77-86.

Kotzekidou, P., Giannakidis, P., & Boulamatsis, A. (2008). Antimicrobial activity of some plant extracts and essential oils against foodborne pathogens in vitro and on the fate of inoculated pathogens in chocolate. *LWT-Food Science and Technology,* 41(1), 119-127.

Kuppan, P., Sethuraman, S., & Krishnan, U. M. (2013). PCL and PCL-gelatin nanofibers as esophageal tissue scaffolds: optimization, characterization and cell-matrix interactions. J Biomed Nanotechnol, 9(9), 1540-55.

Kayaci, F., Sen, H. S., Durgun, E., & Uyar, T. (2014). Functional electrospun polymeric nanofibers incorporating geraniol-cyclodextrin inclusion complexes: High thermal stability and enhanced durability of geraniol. *Food Research International*. https://doi.org/10.1016/j.foodres.2014.03.033

Labet, M., & Thielemans, W. (2009). Synthesis of polycaprolactone: a review. *Chemical society reviews,* 38(12), 3484-3504.

Lin, L., Zhu, Y., & Cui, H. (2018). Electrospun thyme essential oil/gelatin nanofibers for active packaging against Campylobacter jejuni in chicken. *Lwt,* 97, 711-718.

Macosko, C. W., & Krieger, I. M. (1996). Rheology: Principles, Measurements, and Applications. J*ournal of Colloid and Interface Science*, 178(1), 382.

Mahmood, K., Kamilah, H., Sudesh, K., Karim, A. A., & Ariffin, F. (2019). Study of electrospun fish gelatin nanofilms from benign organic acids as solvents. *Food Packaging and Shelf Life,* 19, 66-75.

Mendes, A. C., Stephansen, K., & Chronakis, I. S. (2017). Electrospinning of food proteins and polysaccharides. *Food Hydrocolloids,* 68, 53-68.

Mirghani, M. E. S., Liyana, Y., & Parveen, J. (2012). Bioactivity analysis of lemongrass (Cymbopogan citratus) essential oil. *International Food Research Journal,* 19(2), 569.

Naik, M. I., Fomda, B. A., Jaykumar, E., & Bhat, J. A. (2010). Antibacterial activity of lemongrass (Cymbopogon citratus) oil against some selected pathogenic bacterias. *Asian Pacific Journal of Tropical Medicine*. https://doi.org/10.1016/S1995-7645(10)60129-0

Noori, S., Zeynali, F., & Almasi, H. (2018). Antimicrobial and antioxidant efficiency of nanoemulsion-based edible coating containing ginger (Zingiber officinale) essential oil and its effect on safety and quality attributes of chicken breast fillets. *Food control*, 84, 312-320.

Okutan, N., Terzi, P., & Altay, F. (2014). Affecting parameters on electrospinning process and characterization of electrospun gelatin nanofibers. *Food Hydrocolloids*, 39, 19-26.

Oyedele, A. O., Gbolade, A. A., Sosan, M. B., Adewoyin, F. B., Soyelu, O. L., & Orafidiya, O. O. (2002). Formulation of an effective mosquito-repellent topical product from lemongrass oil. *Phytomedicine,* 9(3), 259-262.

Park, J. S. (2011). Electrospinning and its applications. *Advances in Natural Sciences:*

Nanoscience and Nanotechnology, 1(4), 043002.

Poshadri, A., & Aparna, K. (2010). Microencapsulation technology: a review. *Journal of Research ANGRAU,* 38(1), 86-102.

Ramos, M., Valdes, A., Beltran, A., & Garrigós, M. C. (2016). Gelatin-based films and coatings for food packaging applications. *Coatings,* 6(4), 41.

Rao, J., Chen, B., & McClements, D. J. (2019). Improving the efficacy of essential oils as antimicrobials in foods: Mechanisms of action. *Annual review of food science and technology,* 10, 365-387.

Rieger, K. A., & Schiffman, J. D. (2014). Electrospinning an essential oil: Cinnamaldehyde enhances the antimicrobial efficacy of chitosan/poly (ethylene oxide) nanofibers. *Carbohydrate polymers,* 113, 561-568.

Riquelme, N., Herrera, M. L., & Matiacevich, S. (2017). Active films based on alginate containing lemongrass essential oil encapsulated: Effect of process and storage conditions. *Food and Bioproducts Processing*, *104*, 94–103. https://doi.org/10.1016/j.fbp.2017.05.005

Rutledge, G. C., & Fridrikh, S. V. (2007). Formation of fibers by electrospinning. *Advanced drug delivery reviews*, 59(14), 1384-1391.

Saikia, D., Khanuja, S. P., Kahol, A. P., Gupta, S. C., & Kumar, S. (2001). Comparative antifungal activity of essential oils and constituents from three distinct genotypes of Cymbopogon spp. *Current Science,* 80(10), 1264-1266.

Salvia-Trujillo, L., Rojas-Graü, M. A., Soliva-Fortuny, R., & Martin-Belloso, O. (2014). Impact of microfluidization or ultrasound processing on the antimicrobial activity against Escherichia coli of lemongrass oil-loaded nanoemulsions. *Food Control,* 37, 292-297.

Salević, A., Prieto, C., Cabedo, L., Nedović, V., & Lagaron, J. M. (2019). Physicochemical, antioxidant and antimicrobial properties of electrospun poly (ε-caprolactone) films containing a solid dispersion of sage (Salvia officinalis L.) extract. *Nanomaterials,* 9(2), 270.

Sánchez-González, L., Vargas, M., González-Martínez, C., Chiralt, A., & Chafer, M.

(2011). Use of essential oils in bioactive edible coatings: a review. *Food Engineering Reviews,* 3(1), 1-16.

Schiffman, J. D., & Schauer, C. L. (2008). A review: electrospinning of biopolymer nanofibers and their applications. *Polymer reviews,* 48(2), 317-352.

Shahbazi, Y., Karami, N., & Shavisi, N. (2018). Effect of Ziziphora clinopodioides essential oil on shelf life and fate of Listeria monocytogenes and Staphylococcus aureus in refrigerated chicken meatballs. *Journal of Food Safety*, 38(1), e12394.

Shahidi, F., & Han, X. Q. (1993). Encapsulation of Food Ingredients. *Critical Reviews in Food Science and Nutrition*, *33*(6), 501–547. https://doi.org/10.1080/10408399309527645

Shuiping, L., Lianjiang, T., Weili, H., Xiaoqiang, L., & Yanmo, C. (2010). Cellulose acetate nanofibers with photochromic property: Fabrication and characterization. *Materials Letters,* 64(22), 2427-2430.

Singh, B. R., Singh, V., Singh, R. K., & Ebibeni, N. (2011). Antimicrobial activity of lemongrass (Cymbopogon citratus) oil against microbes of environmental, clinical and food origin. *Int Res J Pharm Pharmacol,* 1(9), 228-236.

Sill, T. J., & Von Recum, H. A. (2008). Electrospinning: applications in drug delivery and tissue engineering. *Biomaterials,* 29(13), 1989-2006.

Silva da, F. T., da Cunha, K. F., Fonseca, L. M., Antunes, M. D., El Halal, S. L. M., Fiorentini, Â. M., ... & Dias, A. R. G. (2018). Action of ginger essential oil (Zingiber officinale) encapsulated in proteins ultrafine fibers on the antimicrobial control in situ. *International journal of biological macromolecules,* 118, 107-115.

Son, W. K., Youk, J. H., Lee, T. S., & Park, W. H. (2004). The effects of solution properties and polyelectrolyte on electrospinning of ultrafine poly (ethylene oxide) *fibers. polymer*, 45(9), 2959-2966.

Soysal, Ç., Bozkurt, H., Dirican, E., Güçlü, M., Bozhüyük, E. D., Uslu, A. E., & Kaya, S. (2015). Effect of antimicrobial packaging on physicochemical and microbial quality of chicken drumsticks. *Food Control,* 54, 294-299.

Subbiah, T., Bhat, G. S., Tock, R. W., Parameswaran, S., & Ramkumar, S. S. (2005).

Electrospinning of nanofibers. *Journal of applied polymer science,* 96(2), 557-569.

Suman, S. P., & Joseph, P. (2013). Myoglobin chemistry and meat color. *Annual review of food science and technology,* 4, 79-99.

Tang, Y., Zhou, Y., Lan, X., Huang, D., Luo, T., Ji, J., … Wang, W. (2019). Electrospun Gelatin Nanofibers Encapsulated with Peppermint and Chamomile Essential Oils as Potential Edible Packaging. *Journal of Agricultural and Food Chemistry*. https://doi.org/10.1021/acs.jafc.8b06226

Tavassoli-Kafrani, E., Goli, S. A. H., & Fathi, M. (2018). Encapsulation of orange essential oil using cross-linked electrospun gelatin nanofibers. *Food and bioprocess technology,* 11(2), 427-434.

Tian, M., Hu, Q., Wu, H., Zhang, L., Fong, H., & Zhang, L. (2011). Formation and morphological stability of polybutadiene rubber fibers prepared through combination of electrospinning and in-situ photo-crosslinking. *Materials Letters*, 65(19-20), 3076-3079.

Torres-Giner, S. (2011). Electrospun nanofibers for food packaging applications. In *Multifunctional and Nanoreinforced Polymers for Food Packaging* (pp. 108–125). Elsevier. https://doi.org/10.1533/9780857092786.1.108

Tucker, N., Stanger, J. J., Staiger, M. P., Razzaq, H., & Hofman, K. (2012). The *history of the science and technology of electrospinning from 1600 to 1995. Journal of engineered fibers and fabrics*, 7(2_suppl), 155892501200702S10.

Tzortzakis, N. G., & Economakis, C. D. (2007). Antifungal activity of lemongrass (Cympopogon citratus L.) essential oil against key postharvest pathogens. *Innovative Food Science & Emerging Technologies,* 8(2), 253-258.

Vafania, B., Fathi, M., & Soleimanian-Zad, S. (2019). Nanoencapsulation of thyme essential oil in chitosan-gelatin nanofibers by nozzle-less electrospinning and their application to reduce nitrite in sausages. *Food and bioproducts processing,* 116, 240-248.

Van der Schueren, L., De Schoenmaker, B., Kalaoglu, Ö. I., & De Clerck, K. (2011). An alternative solvent system for the steady state electrospinning of polycaprolactone. *European Polymer Journal,* 47(6), 1256-1263.

Vilela, J., Martins, D., Monteiro-Silva, F., González-Aguilar, G., de Almeida, J. M., & Saraiva, C. (2016). Antimicrobial effect of essential oils of Laurus nobilis L. and Rosmarinus officinallis L. on shelf-life of minced "Maronesa" beef stored under different packaging conditions. *Food Packaging and Shelf Life,* 8, 71-80.

Vishwakarma, G. S., Gautam, N., Babu, J. N., Mittal, S., & Jaitak, V. (2016). Polymeric encapsulates of essential oils and their constituents: A review of preparation techniques, characterization, and sustainable release mechanisms. *Polymer reviews,* 56(4), 668-701.

Wang, Y., Liu, A., Ye, R., Li, X., Han, Y., & Liu, C. (2015). The production of gelatin-calcium carbonate composite films with different antioxidants. *International Journal of Food Properties,* 18(11), 2442-2456.

Wen, P., Zong, M. H., Linhardt, R. J., Feng, K., & Wu, H. (2017). Electrospinning: A novel nano-encapsulation approach for bioactive compounds. *Trends in Food Science and Technology*. https://doi.org/10.1016/j.tifs.2017.10.009

Wu, J., Sun, X., Guo, X., Ge, S., & Zhang, Q. (2017). Physicochemical properties, antimicrobial activity and oil release of fish gelatin films incorporated with cinnamon essential oil. *Aquaculture and Fisheries,* 2(4), 185-192.

Yao, Z. C., Chang, M. W., Ahmad, Z., & Li, J. S. (2016). Encapsulation of rose hip seed oil into fibrous zein films for ambient and on demand food preservation via coaxial electrospinning. *Journal of Food Engineering*. https://doi.org/10.1016/j.jfoodeng.2016.07.012

Yarin, A. L., Koombhongse, S., & Reneker, D. H. (2001). Taylor cone and jetting from liquid droplets in electrospinning of nanofibers. *Journal of applied physics,* 90(9), 4836-4846.

Yashaswini, M., & Iyer, P. (2019). Chitosan Based Films Incorporated with Turmeric/Clove/Ginger Essential Oil for Food Packaging. *J Nanomed Nanotech,* 10, 537.Madene, A., Jacquot, M., Scher, J., & Desobry, S. (2006). Flavour

encapsulation and controlled release - A review. *International Journal of Food Science and Technology*, *41*(1), 1–21. https://doi.org/10.1111/j.1365-2621.2005.00980.x

Yu, D. G., Williams, G. R., Gao, L. D., Bligh, S. A., Yang, J. H., & Wang, X. (2012). Coaxial electrospinning with sodium dodecylbenzene sulfonate solution for high quality polyacrylonitrile nanofibers. *Colloids and Surfaces A: Physicochemical and Engineering Aspects,* 396, 161-168.

Zhang, C., Li, Y., Wang, P., & Zhang, H. (2020, March 1). Electrospinning of nanofibers: Potentials and perspectives for active food packaging. *Comprehensive Reviews in Food Science and Food Safety*. Blackwell Publishing Inc. https://doi.org/10.1111/1541-4337.12536

Zhang, C., Yuan, X., Wu, L., Han, Y., & Sheng, J. (2005). Study on morphology of electrospun poly (vinyl alcohol) mats. *European polymer journal,* 41(3), 423-432.

Zhang, Y. Z., Venugopal, J., Huang, Z. M., Lim, C. T., & Ramakrishna, S. (2006). Crosslinking of the electrospun gelatin nanofibers. *Polymer,* 47(8), 2911-2917.

Ziğal, N. (2012). Nanolif kaplı kuvars kristal mikroterazi yüzeyler ile kütle hassas biyosensörlerin performansının geliştirilmesi. Fen Bilimleri Enstitüsü.

Zong, X., Kim, K., Fang, D., Ran, S., Hsiao, B. S., & Chu, B. (2002). Structure and process relationship of electrospun bioabsorbable nanofiber membranes. *Polymer,* 43(16), 4403-4412.

A

Significance of the Experimental Design

3 Factors: A, B, C

Design Matrix Evaluation for Combined Quadratic x Quadratic Model
***** Mixture Component Coding is L_Pseudo. *****

Degrees of Freedom for Evaluation

Model	8
Residuals	10
Lack 0f Fit	*5*
Pure Error	*5*
Corr Total	18

A recommendation is a minimum of 3 lack of fit df and 4 df for pure error. This ensures a valid lack of fit test. Fewer df will lead to a test that may not detect lack of fit.

Term	StdErr**	VIF	Ri-Squared	Power at 5 % alpha level for effect of 0.5 Std. Dev.	1 Std. Dev.2 Std. Dev.
A	0.776	4.97	0.7996.8 %	12.2 %	34.4 %
B	0.934	6.33	0.8426.8 %	12.2 %	34.4 %
AB	4.03	6.33	0.8427.4 %	14.7 %	43.5 %
AC	0.486	1.25	0.2027.5 %	15.4 %	46.1 %
BC	0.495	1.24	0.1957.4 %	15.0 %	44.6 %
ABC	2.67	1.59	0.3696.3 %	10.4 %	27.4 %
AC^2	0.957	4.48	0.7777.6 %	15.7 %	47.2 %
BC^2	1.07	5.52	0.8197.1 %	13.6 %	39.4 %
ABC^2	5.09	5.08	0.8036.5 %	11.0 %	29.6 %

****Basis Std. Dev. = 1.0**
Response 1 R1

ANOVA for Combined Quadratic x Quadratic Model
***** Mixture Component Coding is L_Pseudo. *****
Analysis of variance table [Partial sum of squares - Type III]

Source	Sum of Squares	df	Mean Square	F Value	p-value Prob > F
Model	3.27E+004	8	4.09E+003	17.1	< 0.0001
significant					
Linear Mixture	*48.9*	*1*	*48.9*	*0.205*	*0.661*
AB0.608	*1*	*0.608*	*0.00255*	*0.961*	
AC8.90E+003	*1*	*8.90E+003*	*37.3*	*0.000115*	
BC9.57E+003	*1*	*9.57E+003*	*40.1*	*< 0.0001*	
ABC138.	*1*	*138.*	*0.576*	*0.465*	
AC²4.18E+003	*1*	*4.18E+003*	*17.5*	*0.00188*	
BC²2.19E+003	*1*	*2.19E+003*	*9.18*	*0.0127*	
ABC²11.6	*1*	*11.6*	*0.0484*	*0.830*	
Residual	2.39E+003	10	239.		
Lack of Fit	*2.39E+003*	*5*	*478.*	*3.41E+004*	*< 0.0001*
significant					
Pure Error	*0.0700*	*5*	*0.0140*		
Cor Total	3.51E+004	18			

The Model F-value of 3.52 implies the model is significant. There is only a 3.33% chance that a "Model F-Value" this large could occur due to noise.

Values of "Prob > F" less than 0.0500 indicate model terms are significant. In this case ABC are significant model terms. Values greater than 0.1000 indicate the model terms are not significant. If there are many insignificant model terms (not counting those required to support hierarchy), model reduction may improve your model.

The "Lack of Fit F-value" of 37.53 implies the Lack of Fit is significant. There is only a 0.06% chance that a "Lack of Fit F-value" this large could occur due to noise. Significant lack of fit is bad -- we want the model to fit.

Std. Dev.	37.0	R-Squared	0.738
Mean	148.	Adj R-Squared	0.528
C.V. %	25.0	Pred	Squared
0.0995PRESS	5.74E+004	Adeq Precision	6.69

A negative "Pred R-Squared" implies that the overall mean is a better predictor of your response than the current model. "Adeq Precision" measures the signal to noise ratio. A ratio greater than 4 is desirable. Our ratio of 6.687 indicates an adequate signal. This model can be used to navigate the design space.

Coefficient Component	Estimate	Standard df	95% CI Error	95% CI Low	High	VIF
A-A113.	1	12.0	85.9	139.	4.97	
B-B99.9	1	14.4	67.7	132.	6.33	
AB-3.14	1	62.2	-142.	135.	6.33	
AC45.8	1	7.50	29.1	62.5	1.25	
BC48.5	1	7.66	31.4	65.5	1.24	
ABC	-31.3	1	41.2	-123.	60.6	1.59
AC^2-61.9	1	14.8	-94.8	-28.9	4.48	
BC^2-50.1	1	16.5	-86.9	-13.3	5.52	
ABC^2	17.3	1	78.6	-158.	192.	5.08

Final Equation in Terms of L_Pseudo Components and Coded Factors:

R1	=
181.	* A
152.	* B
77.2	* A * B
0.563	* A * C
13.4	* B * C
-359.	* A * B * C
-66.5	* A * C^2
-35.8	* B * C^2
222.	* A * B * C^2

Final Equation in Terms of Real Components and Actual Factors:

R1	=
114.	* A
103.	* B
658.	* A * B
267.	* A * C
170.	* B * C
-1.61E+003	* A * B * C
-266.	* A * C^2
-143.	* B * C^2
888.	* A * B * C^2

Final Equation in Terms of Actual Components and Actual Factors:

R1	=
114.	* A
103.	* B
658.	* A * B
267.	* A * C
170.	* B * C
-1.61E+003	* A * B * C
-266.	* A * C^2
-143.	* B * C^2
888.	* A * B * C^2

Response 2 R2

ANOVA for Combined Quadratic x Quadratic Model * Mixture Component Coding is L_Pseudo. *****

Analysis of variance table [Partial sum of squares - Type III]

Source	Sum of Squares	df	Mean Square	F Value	p-value Prob > F
Model significant	3.27E+004	8	4.09E+003	17.1	< 0.0001
Linear Mixture	*48.9*	*1*	*48.9*	*0.205*	*0.661*
AB0.608	*1*	*0.608*	*0.00255*	*0.961*	
AC8.90E+003	*1*	*8.90E+003*	*37.3*	*0.000115*	
BC9.57E+003	*1*	*9.57E+003*	*40.1*	*< 0.0001*	
ABC138.	*1*	*138.*	*0.576*	*0.465*	
$AC^2$4.18E+003	*1*	*4.18E+003*	*17.5*	*0.00188*	
$BC^2$2.19E+003	*1*	*2.19E+003*	*9.18*	*0.0127*	
$ABC^2$11.6	*1*	*11.6*	*0.0484*	*0.830*	
Residual	2.39E+003	10	239.		
Lack of Fit significant	*2.39E+003*	*5*	*478.*	*3.41E+004*	*< 0.0001*
Pure Error	*0.0700*	*5*	*0.0140*		
Cor Total	3.51E+004	18			

The Model F-value of 17.13 implies the model is significant. There is only a 0.01% chance that a "Model F-Value" this large could occur due to noise. Values of "Prob > F" less than 0.0500 indicate model terms are significant. In this case AC, BC, AC^2, BC^2 are significant model terms. Values greater than 0.1000 indicate the model terms are not significant. If there are many insignificant model terms (not counting those required to supporthierarchy),model reduction may improve your model. The "Lack of Fit F-value" of 34113.65 implies the Lack of Fit is significant. There is

only a 0.01% chance that a "Lack of Fit F-value" this large could occur due to noise. Significant lack of fit is bad -- we want the model to fit.

Std. Dev.	15.5	R-Squared	0.932
Mean	71.9	Adj R-Squared	0.878
C.V. %	21.5	Pred R-Squared	0.465
PRESS	1.88E+004	Adeq Precision	10.7

The "Pred R-Squared" of 0.4653 is not as close to the "Adj R-Squared" of 0.8776 as one might normally expect. This may indicate a large block effect or a possible problem with your model and/or data. Things to consider are model reduction, response tranformation, outliers, etc.

"Adeq Precision" measures the signal to noise ratio. A ratio greater than 4 is desirable. Your ratio of 10.713 indicates an adequate signal. This model can be used to navigate the design space.

Coefficient Component	Estimate	Standard df	95% CI Error	95% CI Low	High	VIF
A-A113.	1	12.0	85.9	139.	4.97	
B-B99.9	1	14.4	67.7	132.	6.33	
AB-3.14	1	62.2	-142.	135.	6.33	
AC45.8	1	7.50	29.1	62.5	1.25	
BC48.5	1	7.66	31.4	65.5	1.24	
ABC	-31.3	1	41.2	-123.	60.6	1.59
AC^2-61.9	1	14.8	-94.8	-28.9	4.48	
BC^2-50.1	1	16.5	-86.9	-13.3	5.52	
ABC^2	17.3	1	78.6	-158.	192.	5.08

Final Equation in Terms of L_Pseudo Components and Coded Factors:

R2	=
113.	* A
99.9	* B
-3.14	* A * B
45.8	* A * C
48.5	* B * C
-31.3	* A * B * C
-61.9	* A * C^2
-50.1	* B * C^2
17.3	* A * B * C^2

Final Equation in Terms of Real Components and Actual Factors:

R2	=
4.99	* A
1.32	* B
45.5	* A * B
339.	* A * C
297.	* B * C
-132.	* A * B * C
-247.	* A * C^2
-200.	* B * C^2
69.2	* A * B * C^2

Final Equation in Terms of Actual Components and Actual Factors:

R2	=
4.99	* A
1.32	* B
45.5	* A * B
339.	* A * C
297.	* B * C
-132.	* A * B * C
-247.	* A * C^2
-200.	* B * C^2
69.2	* A * B * C^2

PUBLICATIONS FROM THE THESIS

Papers

1. Can, F.O. & Durak, M. Z. Encapsulation of Lemongrass Oil for Antimicrobial and Biodegradable Food Packaging Applications. *Science of Advanced Material*, (to be published).